Biogeosciences Discuss., 11, 16645–16701, 2014
www.biogeosciences-discuss.net/11/16645/2014/
doi:10.5194/bgd-11-16645-2014

Biogeosciences Discussions
Open Access

Flux variations and vertical distributions of microzooplankton (Radiolaria) in the western Arctic Ocean: environmental indices in a warming Arctic

T. Ikenoue[1,2,3,*], K. R. Bjørklund[2], S. B. Kruglikova[4], J. Onodera[3], K. Kimoto[3], and N. Harada[3]

[1]Department of Earth and Planetary Sciences, Graduate School of Sciences, Kyushu University, 6-10-1 Hakozaki, Higashi-ku, Fukuoka 812-8581, Japan
[2]Natural History Museum, Department of Geology, University of Oslo, P.O. Box 1172 Blindern, 0318 Oslo, Norway
[3]Research and Development Center for Global Change, JAMSTEC, Natsushima-cho 2-15, Yokosuka, 237-0061, Japan
[4]P.P. Shirshov Institute of Oceanology, Russian Academy of Sciences, Nakhimovsky Prospect 36, 117883 Moscow, Russia
[*]now at: Central Laboratory, Marine Ecology Research Institute, 300 Iwawada, Onjuku-machi, Isumi-gun, Chiba 299-5105 Japan

Received: 4 October 2014 – Accepted: 10 November 2014 – Published: 3 December 2014

Correspondence to: T. Ikenoue (ikenoue@kaiseiken.or.jp)

Published by Copernicus Publications on behalf of the European Geosciences Union.

Abstract

The vertical distribution of radiolarians was investigated using a vertical multiple plankton sampler (100–0, 250–100, 500–250 and 1000–500 m water depths, 62 µm mesh size) at the Northwind Abyssal Plain and southwestern Canada Basin in September 2013. To investigate seasonal variations in the flux of radiolarians in relation to sea-ice and water masses, time series sediment trap system was moored at Station NAP (75°00′ N, 162°00′ W, bottom depth 1975 m) in the western Arctic Ocean during October 2010–September 2012. We showed characteristics of fourteen abundant radiolarian taxa related to the vertical hydrographic structure in the western Arctic Ocean. We found the *Ceratocyrtis histricosus*, a warm Atlantic water species, in net samples, indicating that it has extended its habitat into the Pacific Winter Water. The radiolarian flux was comparable to that in the North Pacific Oceans. *Amphimelissa setosa* was dominant during the open water and the beginning and the end of ice cover seasons with well-grown ice algae, ice fauna and with alternation of stable water masses and deep vertical mixing. During the sea-ice cover season, however, oligotrophic and cold-water tolerant Actinommidae was dominant and the productivity of radiolaria was lower and its species diversity was greater, which might be associated with the seasonal increase of solar radiation that induce the growth of algae on the ice and the other phytoplankton species under the sea-ice. These indicated that the dynamics of sea-ice was a major factor affecting the productivity, distribution, and composition of radiolarian fauna.

1 Introduction

In recent years, summer sea-ice extent in the Arctic Ocean decreases rapidly due to global climate change (Stroeve et al., 2007, 2012). The sea-ice in the Arctic Ocean reached the minimum extent in September 2012 since the beginning of satellite observation (NSIDC, 2012). The most remarkable sea-ice decrease was observed in the

western Arctic Ocean of the Pacific side (Shimada et al., 2006; Comiso et al., 2008; Markus et al., 2009). In the western Arctic Ocean, the warm pacific water through the Bering Strait contributes to both sea-ice melt in summer and an inhibition of sea-ice formation during winter (Shimada et al., 2006; Itoh et al., 2013).

The biological CO_2 absorption is an important carbon sink in the area without sea-ice in the Arctic Ocean (Bates et al., 2006; Bates and Mathis, 2009). Melting of sea-ice can both enhance and reduce the biological pump in the Arctic Ocean, depending on ocean circulation (Nishino et al., 2011). The Beaufort High, a high pressure over the Canada Basin in the Arctic Ocean, drives the sea-ice and the water masses anticyclonically, as the Beaufort Gyre (Fig. 1). In the Canada Basin, the Beaufort Gyre governs the upper ocean circulation (Proshutinsky et al., 2002). The Beaufort Gyre has been become enhanced recently due to the decreasing sea-ice (Shimada et al., 2006; Yang, 2009). The biological pump is reduced within the Beaufort Gyre, and conversely, it is enhanced outside the Beaufort Gyre (Nishino et al., 2011).

Particle flux play important roles in the carbon export (Francois et al., 2002). With the samples collected by sediment trap in the Canada Basin and Chukchi Rise, Honjo et al. (2010) found that annual average of sinking particle flux was three orders of magnitude smaller than that in epipelagic areas where the particle flux represented an important role for carbon export to greater depths. However, Arrigo et al. (2012) observed a massive algal biomass beneath fully consolidated pack ice far from the ice edge in the Chukchi Sea during the summer, and suggested that a thinning ice cover increased light transmission under the ice and allowed blooming of algae. Boetius et al. (2013) also reported that the algal biomass released from the melting ice in the Arctic Ocean was widely deposited at the sea floor in the summer of 2012. Therefore, it is inferred that biomass of zooplankton also changed seasonally under the sea-ice in the Arctic Ocean, as a result of the variable sea-ice conditions. Microzooplankton are now recognized as a key component of pelagic food webs (e.g., Calbet and Landry, 2004). The seasonal and interannual changes of microzooplankton communities within the sea ice regions, however, are still poorly understood.

To understand the effect of sea ice reduction on marine ecosystems in the Arctic Ocean, we studied productivity, distribution, composition, and biological regime of living radiolarians, which are one of the commonest micro-zooplankton groups that secrete siliceous skeletons, based on the plankton tow samples and sediment trap samples.

The abundance of microzooplankton radiolaria in a region is related to temperature, salinity, productivity and nutrient availability (Anderson, 1983; Bjørklund et al., 1998; Cortese and Bjørklund, 1997; Cortese et al., 2003). Not only at species level but also at genus and family levels radiolarians represent various oceanographic conditions by their distribution patterns and compositions (Kruglikova et al., 2010, 2011). In recent studies, Ikenoue et al. (2012a, b) found a close relationship between water mass exchanges and radiolarian abundances based on a fifteen year long time-series observation on radiolarian fluxes in the central subarctic Pacific. Radiolarian assemblages are also related to the vertical hydrographic structure (e.g., Kling, 1979; Ishitani and Takahashi, 2007; Boltovskoy et al., 2010), therefore variations in their abundance and proportion might be useful environmental proxies for water mass exchanges at each depth interval related to the recent climate change (e.g., ocean circulation change, prosperity and decline of sea-ice, influx of water mass from other regions).

The radiolarian assemblages in the western Arctic Ocean has been studied mainly based on the samples collected by plankton net tow at the ice-floe stations (Hülseman 1963; Tibbs, 1967), and in the Beaufort Sea in summer of 2000 (Itaki et al., 2003) or the surface sediment samples mainly over the Atlantic side of the Arctic Ocean (Bjørklund and Kruglikova, 2003). However, the knowledge of the geographical and the depth distribution of living radiolarians are still limited, and the seasonal and annual changes of radiolarians has not been studied in the western Arctic Ocean because of seasonal sea-ice coverage.

This is the first extensive study of the seasonal and interannual flux changes of radiolarians in the western Arctic Ocean. We present radiolarian depth distributions and flux variations in the western Arctic Ocean based on plankton tow samples and sediment trap material, respectively. We discuss their seasonality and species associations in

relation to the environmental conditions (temperature, salinity, depth, sea-ice concentration, and downward shortwave radiation).

2 Oceanographic setting

The hydrography in the western Arctic Ocean has been discussed in several studies (e.g., Aagaard et al., 1985; McLaughlin et al., 2011) and the upper 1000 m of the water column can be divided into five distinct water masses. The surface water is characterized by low temperature and low salinity water (Aagaard et al., 1981) and can be subdivided into three layers, i.e. Surface Mixed Layer (SML), Pacific Summer Water (PSW), Pacific Winter Water (PWW). The SML (0–25 m) is formed in summer by sea-ice melt and river runoff and is characterized by very low salinities (less than 28 psu). The PSW (25–100 m) and PWW (100–250 m) are cold halocline layers originating from the Pacific Ocean via the Bering Sea. The PSW flows along the Alaskan coastal area and enters the Canada Basin through the Bering Strait and Barrow Canyon (Coachman and Barnes, 1961) (Fig. 1). The PSW is relatively warmer and less saline (30–32 psu in the 1990s, 28–32 psu in the 2000s, according to Jackson et al., 2011) than the PWW. The PSW is further classified into warmer and less saline Alaskan coastal water and cooler and more saline Bering Sea water (Coachman et al., 1975), which originate from Pacific water that is modified in the Chukchi and Bering Seas during summer. The Alaskan coastal water is carried by a current along the Alaskan coast, and spread northwards along the Northwind Ridge by the Beaufort gyre depending on the rates of ice cover and decay (Shimada et al., 2001). The PWW is characterized by a temperature minimum (of about $-1.7\,^{\circ}C$) and originates from Pacific water that is modified in the Chukchi and Bering Seas during winter (Coachman and Barnes, 1961). The PWW is also characterized by a nutrient maximum and its source is regenerated nutrients from the shelf sediments (Jones and Anderson, 1986).

The deep water is divided into Atlantic Water (AW), Canada Basin Deep Water (CBDW). AW (250–900 m) is warmer (near or below $1\,^{\circ}C$) and saltier (near 35 psu)

intermediate water than the surface waters, which is originating from the North Atlantic Ocean, via the Norwegian Sea. The CBDW (below 900 m) is a cold (lower than 0 °C) water mass located beneath the AW and has the same salinity as the AW. The CBDW is formed by the brine formation on the shelves, which makes cold and saline water mass sinking over the continental margin into the deep basins (Aagaard et al., 1985).

3 Materials and methods

3.1 Plankton tow samples

Plankton tow samples were collected by vertical multiple plankton sampler (VMPS). VMPS (mesh size: 62 µm, open mouth area: 0.25 m^2) was towed from 4 layers (100–0, 250–100, 500–250, and 1000–500 m) at 2 stations (Station 32 in Northwind Abyssal Plain, 74°32′ N, 161°54′ W; Station 56 in southwestern Canada Basin, 73°48′ N, 159°59′ W) (Fig. 1 and Table 1) in September 2013. Hydrographical data (temperature, salinity) down to 1000 m water depth were simultaneously obtained from a CTD observation with the plankton sampling. The volume of seawater filtered through the net was estimated using a flow meter mounted in the mouth ring of the plankton net.

The samples collected by VMPS were split with a Motoda box splitter and a rotary splitter (McLane™WSD-10). The split samples were fixed with 99.5 % ethanol for radiolarian studies. Plankton samples were stained with Rose-Bengal to discriminate between living and dead specimens. The split samples were sieved through a stainless screen with 45 µm mesh size. Remains on the screen were filtered through Gelman® membrane filters with a nominal pore size of 0.45 µm. The filtered samples were desalted with distilled water and dried, then permanently mounted with Canada Balsam on microslides. Radiolarian taxa were identified and counted with a compound light microscope at 200× or 400× magnification. Phaeodaria have not been recognized as Radiolaria but as Cercozoa in recent studies using molecular biology (Cavalier-Smith

and Chao, 2003; Nikolaev et al., 2004; Adl et al., 2005; Yuasa et al., 2005). To avoid complications we dealt with the phaeodarians as one of the radiolarian groups according to the classical taxonomy (Anderson et al., 2002; Takahashi and Anderson, 2002). We determined that specimens were "living", if their protoplasm was stained clearly, this to avoid false staining by other organisms such as bacterial growth). All specimens on a slide were identified and counted, and their individual numbers were converted to standing stocks (No. specimens m^{-3}).

3.2 Hydrographic profiles

Profiles of temperature, salinity, and dissolved oxygen down to 1000 m depth at stations 32 (Northwind Abyssal Plain) and 56 (southwestern Canada Basin) in September 2013 are from Nishino (2013) and shown in Fig. 2a and b, respectively. At Station 32, temperature showed sharp decrease from the surface and down to about 25 m depth with a sharp increase at the base of SML. The PSW is generally cold (about −1 °C) with a maximum value (1.6 °C) at about 50 m and show a rapid decrease with increasing depth. The PWW is the coldest water (minimum value −1.6 °C) at about 200 m. Highest temperatures are found in the AW (near or below 1 °C) at about 400 m with a gradual decrease below 500 m. Salinity showed low values (25–28 psu) in the SML, increasing rapidly with depth from 28–32 psu in the PSW. In the PWW there is a gradual increase of salinity from 32 to 35 psu, while there is a slight decrease below the PWW/AW boundary. Dissolved oxygen showed maximum value (405 µmol kg^{-1}) at the boundary of the SML and PWW, rapid decrease with increasing depth in the PSW and PWW, minimum value (270 µmol kg^{-1}) around the boundary of the PWW and AW, and slight increase below the boundary of the PWW and AW. Temperature, salinity, and dissolved oxygen show almost similar values at both Station 32 and Station 56 except for in the SML and PSW. In the SML, salinity at Station 32 was slightly lower than at Station 56. In the PSW, a temperature peak at Station 32 was about one degree higher, and a little deeper, compared to Station 56.

3.3 Sediment trap samples

Particle flux samples were collected by a sediment trap (SMD26 S-6000, open mouth area 0.5 m^2, Nichiyu Giken Kogyo, Co. Ltd.) rotated at 10–15 day intervals moored at 184 m (4 October 2010–28 September 2011)–260 m (4 October 2011–18 September 2012) and 1300 m (4 October 2010–28 September 2011)–1360 m (4 October 2011–18 September 2012) at Station NAP (Northwind Abyssal Plain, 75°00′ N, 162°00′ W, bottom depth 1975 m) during 4 October 2010–28 September 2011 and during 4 October 2011–18 September 2012 (Fig. 1; Table 2). The mooring system was designed to set the collecting instrument at approximately 600 m above the sea floor. This depth of the moored sediment traps was chosen in order to avoid possible inclusion of particles from the nepheloid layer, reaching about 400 m above the seafloor (Ewing and Connary, 1970). Recoveries and redeployments of the traps were carried out on the Canadian Coast Guard Ship I/B (ice breaker) *Sir Wilfrid Laurier* and R/V *Mirai* of Japan Agency for Marine–Earth Science and Technology. The sample cups were filled with 5 % buffered formalin seawater before the sediment trap was deployed. This seawater was collected from 1000 m water depth in the southern Canada Basin, and was membrane filtered (0.45 mm pore size). The seawater in the sample cups was mixed with sodium borate as a buffer (pH 7.6–7.8) and 5 % formalin was added as a preservative.

The samples were first sieved through 1 mm mesh to remove larger particles, which are not relevant for the present study. The samples were split with a rotary splitter (McLane^{TM}WSD-10). At first, we used 1/100 aliquot size of the samples to make microslides for microscope work (species identification). We made additional slides in case of low radiolarian specimen numbers. In order to remove organic matter and protoplasm, 20 mL of 10 % hydrogen peroxide solution are added to the samples in a 100 mL pyrex beaker, and heated (not boiling) on a hot plate for one hour. After this reaction was completed, Calgon® (hexametaphosphate, surfactant) solution was added to disaggregate the sample. The treated samples are then sieved through a screen

(45 µm mesh size). Both the coarse (> 45 µm) and fine (< 45µm) fractions are filtered through Gelman membrane filters with a nominal pore size of 0.45 µm and desalted with distilled water. The edge of each filtered samples are cut according to slide size in wet condition and mounted on glass slides on a slide warmer. The dried filters and samples are added Xylene, and permanently mounted with Canada balsam.

We made slides of both the coarse (> 45 µm) and the fine (< 45 µm) fraction of each sample. For the enumeration of radiolarian taxa in this study, we counted all specimens of radiolarian skeletons larger than 45 µm encountered on a slide. Each sample was examined under an Olympus compound light microscope at 200× or 400× magnification for species identification and counting. The radiolarian flux (No. specimens $m^{-2}\,day^{-1}$) was calculated from our count data using the following formula:

$$\text{Flux} = N \cdot V/S/D \quad (1)$$

where N is the counted number of radiolarians, V the aliquot size, S the aperture area of the sediment trap (0.5 m^2), and D the sampling interval (day). Diversity indices using the Shannon–Weaver log-base 2 formula (Shannon and Weaver, 1949) were calculated for total radiolarians

$$H = -P_i \log_2 P_i \quad (2)$$

where H is the diversity index, P is the contribution of species and i is the order of species.

As supplemental environmental data, the moored sediment trap depth and the water temperature (accuracy of +0.28 °C) were monitored every hour (sensor type: ST-26S-T). Moored trap depth for the upper trap was lowered by about 80 m during the second year (about 260 m depth) than during the first year (about 180 m depth). Especially, during July–August in 2012, the moored trap depth was lowered to about 300 m (Fig. S1). Time-series data of sea-ice concentration around Station NAP during the mooring period were calculated from the sea-ice concentration data set (http://iridl.ldeo.columbia.edu/SOURCES/.IGOSS/.nmc/.Reyn_SmithOIv2/, cf. Reynolds et al., 2002).

3.4 Taxonomic note

The species described by Hülsemann (1963) under the name of *Tholospyris gephyristes* certainly is not a Spyridae at all. This species has been accepted as a Spyridae by most workers, but with a closer view this species has no sagittal ring that is typical for the Spyridae. We have therefore tried to evaluate its taxonomic position and have now an understanding that this species better belongs in the family Plagiacanthidae. Based on our microscope and literature studies we at present conclude that this species can be named *Tripodiscium gephyristes*.

4 Results

4.1 Radiolarians collected by plankton tows

A total of 43 radiolarian taxa (12 Spumellaria, 3 Entactinria, 26 Nassellaria, and 2 Phaeodaria) were identified in the plankton tow samples (Table 3). The numbers of individuals for each radiolarian taxa are in Tables S1 (Station 32) and S2 (Station 56).

4.1.1 Standing stocks and diversities of radiolaria

The abundance of living radiolarians at Station 32 was about two times as large as at Station 56 at each depth interval in the upper 500 m, where the abundance of living radiolarians decreased with increasing water depth at both stations (Fig. 2a and b). The abundance of dead radiolarians also decreased with water depth at both stations except for 100–250 m depth at Station 32 (Fig. 2a and b). The abundance of dead radiolarians was generally higher than living radiolarians at both stations except for in the 0–100 m depth at Station 32. The living radiolarian diversity index was low in the 0–100 m depth interval, increased with depth and the maximum at about 400 m, and then slightly decreased below 500 m depth at both stations.

At Station 32, *Amphimelissa setosa* (58 %) and *Amphimelissa setosa* juvenile (22 %) were dominant, and *Joergensenium* sp. A (6 %), *Pseudodictyophimus clevei* (4 %), Actinommidae spp. juvenile forms (3 %), and *Actinomma leptodermum leptodermum* (1 %) were common (Fig. 3a). At Station 56 the Actinommidae spp. juvenile forms (38 %) and *Amphimelissa setosa* (29 %) were dominant, and *Actinomma leptodermum leptodermum* (6 %), *Amphimelissa setosa* juvenile (6 %), *Pseudodictyophimus clevei* (5 %), and *Joergensenium* sp. A (4 %) were common (Fig. 3b). Actinommidae spp. juvenile forms are juvenile forms of *Actinomma leptodermum leptodermum* and *Actinomma boreale*, but we cannot separate between the two.

4.1.2 Vertical distribution of radiolarian species and environment

We selected fourteen abundant radiolarian taxa to show species characteristics related to the vertical hydrographic structure in the western Arctic Ocean (Fig. 4).

Adult and juvenile of *Amphimelissa setosa* were mainly distributed in the 0–250 m depth at both stations. In the 0–100 m depth, Adult and juvenile stages were dominant (70 and 28 %, respectively) at Station 32, and at Station 56 (23 and 7 %, respectively) following the juvenile *Actinomma* spp. (56 %). In the 100–250 m depth, *A. setosa* was the dominant species at both stations. At Station 32, the abundance of *A. setosa* in the 100–250 m depth interval was lower than in the 0–100 m depth, whereas at Station 56, the abundance in the 100–250 m depth was almost the same as in the 0–100 m depth.

Actinommidae spp. juvenile forms and *Actinomma l. leptodermum* were absent in 0–100 m depth at Station 32, but both, especially Actinommidae spp. juvenile forms (56 %) were abundant at Station 56. Both were common in the 100–250 m depth at both stations (8 and 4 %, respectively at Station 32; 14 and 7 %, respectively at Station 56), and decreased abundance in the 250–500 m depth. *Spongotrochus glacialis* was rare in the 0–100 m depth at Station 32 (0.4 %) but common at Station 56 (1.4 %). In deeper layers *S. glacialis* was rare.

Joergensenium sp. A, *Pseudodictyophimus clevei,* and *Actinomma boreale* were abundant in the 100–250 m depth at both stations. *Joergensenium* sp. A was absent

in the 0–100 m depth but abundant in the 100–250 m depth and rare in deeper depths. *Pseudodictyophimus clevei* distributed throughout surface to 1000 m depth, but was rare at Station 32 except for in the 100–250 m. *Actinomma boreale* was rare and mainly distributed in the 100–250 m depth at both stations.

Ceratocyrtis histricosus was mainly distributed in the 250–500 m depth, and occurred also in the 100–250 m depth at both stations. *Tripodiscium gephyristes* was widely distributed below 100 m depth at Station 56, while at Station 32 this species was scarce at all depth layers. *Pseudodictyophimus g. gracilipes* occurred in very low numbers at both stations through the upper 1000 m. *Pseudodictyophimus plathycephalus*, Plagiacanthidae gen. et sp. in det., and *Cycladophora davisiana* were most abundant below 500 m depth at both stations.

4.2 Radiolaria collected by sediment trap

A total of 51 radiolarian taxa (15 Spumellaria, 3 Entactinria, 31 Nassellaria, and 2 Phaeodaria) were identified in the upper and lower sediment trap samples at Station NAP during 4 October 2010–18 September 2012 (Table 3). The number of radiolarians counted in each sample ranged from 8 to 1100 specimens in the upper trap, and from 0 to 2672 specimens in the lower trap (Tables S3 and S4). There were 15 samples with fewer than 100 specimens (2 samples in upper trap, 13 samples in lower trap). Most of the species recognized in our sample materials are shown in Plates 1–9.

4.2.1 Radiolarian flux and diversity in the upper trap

Total radiolarian flux in the upper trap varied from 114 to 14 677 specimens m^{-2} day^{-1} with an annual mean of 2823 specimens m^{-2} day^{-1} (Fig. 5). The highest fluxes were observed during the beginning of sea-ice cover season (November in 2010 and 2011, > 10 000 specimens m^{-2} day^{-1}). The fluxes were higher during the open water season (August–October in 2011, > 5000 specimens m^{-2} day^{-1}) and around the end of sea-ice cover season (July–August in 2011, > 4000 specimens m^{-2} day^{-1}) than those during

the sea-ice cover season (December–June, mostly < 800 specimens m^{-2} day^{-1}). The diversity of radiolarians, however, was high during the sea-ice cover season (> 3) than open water season (< 2) (Fig. 5). The diversity indices were negative correlated with the total radiolarian fluxes (r = 0.91) (Fig. 6).

Species composition varied seasonally. Adult and juvenile *Amphimelissa setosa* were most dominant (90 %) during the sea-ice free season, and the beginning and the end of sea-ice cover season. The juvenile and adult forms were abundant in earlier and later season, respectively (Fig. 7). During the sea-ice cover season, however, Actinommidae spp. juvenile forms (range, 0–51 %; average, 18 %), *Actinomma leptodermum leptodermum* (range, 0–14.6 %; average, 4 %), *Actinomma boreale* (range, 0–33 %; average, 4 %) were dominant. Relatively high percentages of *Pseudodictyophimus clevei*, *Pseudodictyophimus gracilipes*, *Tripodiscium gephyristes* were also observed during the sea-ice cover season.

4.2.2 Radiolarian flux and diversity in the lower trap

Total radiolarian flux in the lower trap varied from 0 to 22 733 specimens m^{-2} day^{-1} with an annual mean of 4828 specimens m^{-2} day^{-1} (Fig. 5). The fluxes were high during October–November both in 2010 and 2011 and during March in 2011 (> 10 000 specimens m^{-2} day^{-1}), while, extremely low (0–80 specimens m^{-2} day^{-1}) during May–September in 2012. Diversity did not change greatly, and increased slightly during May–July 2011, and in April 2012 when the radiolarian fluxes were low. The diversity indices were weakly and negative correlated with the radiolarian fluxes (r = −0.52) (Fig. 6).

Adult and juvenile stages of *Amphimelissa setosa* were dominant throughout the sampling periods (range, 66–92 %; average, 82 %). During July–September 2011, juvenile and adult forms of *A. setosa* were dominant during June–July and August–September, respectively. The relative abundance of *A. setosa* juvenile was slightly increased in 2012 in comparison to 2010 and 2011.

5 Discussion

5.1 Comparison between Arctic and North Pacific Oceans

Biogenic particle flux into the deep sea in the Canada Basin was low due to the low productivity of shell-bearing microplankton, which play an important role in biological pump process (Honjo et al., 2010). However, we observed high radiolarian fluxes (14 677: upper trap, 22 733: lower trap) at Station NAP during the open water season and around the beginning and the end of sea-ice cover season in 2011–2012. The annual means (2823: upper trap, 4823: lower trap) were comparable to those observed in several areas in the North Pacific Ocean (Fig. 8, Table S5). The biogenic opal collected in this study mainly consisted of radiolarians and diatoms, therefore siliceous skeletons of radiolarians and diatoms might play important role to export biogenic silica to the deep Arctic. Relatively high flux of radiolarians in arctic microplankton might contribute to substantial part of the POC flux.

5.2 Characteristic and ongoing speciation of radiolarians in the western Arctic Ocean

Radiolarian fauna in the western Arctic Ocean had a close affinity to the Atlantic fauna, and the family Cannobotryidae and Actinommidae were dominant in the western Arctic Ocean. Petrushevskaya (1979) pointed out that the arctic-boreal radiolarian species known from the Arctic Ocean basins had been originated from the early Postglacial Norwegian Sea polycystine radiolarian fauna. Bjørklund and Kruglikova (2003) concluded that the modern radiolarian fauna in the Arctic Ocean had a close affinity to the Norwegian Sea radiolarian fauna. Inflow of radiolarians with waters from the northern part of the Pacific Ocean is probably negligible since the most abundant and typical radiolarian species in the North Pacific such as *Stylochlamydium venustum*, and *Ceratospyris borealis* are absent in the western Arctic Ocean. In our results the radiolarian fauna in the western Arctic Ocean were characterized by a wide diversity of the family

Actinommidae and high standing stock of *Joergensenium* sp. A in the PWW (Table S6). *Actinomma* morphogroup A (58 specimens), *Actinomma* morphogroup B (57 specimens), *Joergensenium* sp. A (1401 specimens) observed in the western Arctic Ocean in our study have not been reported in other areas in the Arctic Ocean, nor in the North Pacific and in the North Atlantic. Although we could not conclude yet, *Actinomma* morphogroup A and B and *Joergensenium* sp. A might be new species endemic for the western Arctic. Kruglikova et al. (2009) described two new species *Actinomma georgii* and *A. turidae*, and suggested the endemism hypotheses for these two species as a result that radiolarians had been rapidly evolving under the stressful conditions in the Arctic Ocean and that the central Arctic Basin might be the center of an ongoing speciation within the family Actinommidae. Our results might support this hypothesis suggesting that local speciation took place not only in the central Arctic basin, but also in the western Arctic Ocean. This is demonstrated by the occurrence of a new and still undescribed Actinomma species, very similar to *A. boreale*, but different structure of the medullary shells. Also within the radiolarian group Entactinaria, in the genus Joergensenium, one or two undescribed species are found. The reason for radiolarian species speciation in this area is still not understood but we can only speculate that this can be controlled by the harsh environmental stress (Allen and Gilooly, 2006; Kruglikova et al., 2009). The extremely cold water masses under the sea-ice (−1.7 °C) and the always-changing quality of the water masses as affected by the inflowing Pacific water.

5.3 Vertical distribution of species and hydrographic structure

5.3.1 PSW and PWW association

Amphimelissa setosa and its juvenile stages were found in a shallow cold-water in both stations 32 and 56. Specifically, they were more abundant in the SML and PSW (0–100 m) at Station 32 than Station 56. At Station 32, these two water masses exhibited warmer temperature than Station 56; indicating that cold but moderate warm, and well

mixed water mass were more favorable for this species than the perennial cold water mass such as PWW (100–250 m). The vertical and geographic distribution of *A. setosa* has been described in several previous studies. *Amphimelissa setosa* dominated (60–80 %) the radiolarian assemblage through the upper 500 m of the water column in the Chukchi Sea and the Beaufort Sea and so can be an indicator of cold Arctic surface water (Itaki et al., 2003). Matul and Abelmann (2005) also suggested that *A. setosa* prefers well-mixed, cold and saline surface/subsurface waters.

Actinommidae spp. juvenile forms, *Actinomma l. leptodermum*, *Spongotrochus glacialis* were mainly distributed in the PSW and PWW and preferred different water masses from *Amphimelissa setosa*. *Actinomma l. leptodermum* and *Actinomma boreale* had been reported as a group (e.g. Samtleben et al., 1995), due to identification problems, particularly of the juvenile stages, but the adult stages can be separated into two species following Cortese and Bjørklund (1998). *Actinomma l. leptodermum* were absent in the water masses of SML and PSW at Station 32, but they were abundant in these water masses at Station 56. At Station 56, SML and PSW water masses were colder and more homogeneous than at Station 32; indicating that Actinommidae spp. juvenile forms and *A. l. leptodermum* preferred cold but warmer water than PWW. Small spumellarians might be herbivorous (Anderson, 1983) so Actinommidae spp. juvenile forms and *A. l. leptodermum* might therefore be bound to the euphotic zone where phytoplankton prevails. *Spongotrochus glacialis* showed a similar vertical distribution as Actinommidae spp. juvenile forms and *Actinomma l. leptodermum*. *Spongotrochus glacialis* preferred warmer water than PWW. *Spongotrochus glacialis* inhabited surface water also in the Okhotsk Sea and well adapted to low temperatures and low salinities (Nimmergut and Abelmann, 2002). Okazaki et al. (2004) also reported *S. glacialis* as a subsurface dweller with abundance maximum in the 50–100 m interval in the Okhotsk Sea, associated with the phytoplankton production.

5.3.2 PWW association

Joergensenium sp. A, *Pseudodictyophimus clevei*, and *Actinomma boreale,* were mainly distributed in the PWW. *Joergensenium* sp. A and *P. clevei* might prefer cold water (−1.7 °C) with low turbulence. The depth distribution of *Joergensenium* sp. A were restricted to the PWW (100–250 m) and the upper AW (250–500 m), but *P. clevei* were more flexible and widely distributed. *Joergensenium* sp. A has not yet been described from recent radiolarian assemblages, so can be suggested that *Joergensenium* sp. A might occur only on the Pacific side of the Arctic Ocean and might serve as an indicator for the PWW layer. Standing stocks of *A. boreale* was lower than Actinommidae spp. juvenile forms and *A. l. leptodermum* at both stations, and mainly occurred in the PWW. In the surface sediments of the Greenland, Iceland and Norwegian Seas, *A. boreale* is associated with warm (Atlantic) water, whereas *A. l. leptodermum* is associated with the cold East Greenland Current and the warm Norwegian Current water (Bjørklund et al., 1998). Other environmental factors such as salinity, food availability, or seasonal differences of their growth stages due to the sampling period might be related to the standing stocks of *A. boreale*.

5.3.3 Upper AW association

Ceratocyrtis histricosus occurred commonly in the upper AW (250–500 m) and rarely in the PWW. *Ceratocyrtis histricosus* is a species interpreted as being introduced from the Norwegian Sea, most likely during the early Holocene by the warm Atlantic water drifting through the Arctic Ocean (Kruglikova, 1999). This species has not been observed in the Canada Basin during the 1950s and 1960s (Hülseman 1963; Tibbs, 1967). Furthermore, *C. histricosus* was not reported in the PWW from the plankton samples in the Chukchi and Beaufort Seas in 2000 (Itaki et al., 2003). Itaki et al. (2003) indicated that the occurrence of *C. histricosus* in recent years in the western Arctic Ocean, as we found, was related to the recent warming of the Arctic water. According to McLaughlin et al. (2011), the mean temperature of the PWW within the Canada Basin increased

slightly (~ 0.05 °C) from 2003 to 2007 and then remained constant until 2010. Thus, the recent warming of the PWW and AW might induce the expansion of the habitat of *C. histricosus* into the PWW.

Bjørklund et al. (2012) reported 98 tropical-subtropical radiolarian taxa in the area north of Svalbard in the eastern Arctic Ocean. They stated that there are always pulses of warm Atlantic water that do reach the Arctic Ocean, transporting warmer water fauna. We did not observe any tropical and subtropical radiolarian taxa in the western Arctic Ocean. However, it is necessary to conduct continuous monitoring of the annual changes in the radiolarian fauna, including *C. histricosus*, in the western Arctic Ocean.

5.3.4 Lower AW association

Pseudodictyophimus plathycephalus, Plagiacanthidae gen. et sp. in det., and *Cycladophora davisiana* were abundant in the cold and oxygenated lower AW at both stations. However, their distribution patterns in PWW and upper AW water masses were slightly different between Station 32 and Station 56 whereas temperature, salinity, and dissolved oxygen have similar values at both stations. Their standing stocks might therefore reflect not only hydrographic conditions. *Pseudodictyophimus g. gracilipes* is widely distributed in the world ocean, and known to inhabit the surface layer at high latitudes and at greater depth at low latitudes (Ishitani and Takahashi, 2007; Ishitani et al., 2008). Itaki et al. (2003) reported that the maximum depth of *P. g. gracilipes* occurred at 0–50 m in the Chukchi Sea and 25–50 m in the Beaufort Sea. However, in our results, *P. g. gracilipes* did not show any specific vertical distribution, and its standing stocks were low.

5.4 Seasonal and annual radiolarian flux

5.4.1 Radiolarian fauna and seasonal sea-ice concentration

Seasonal radiolarian fluxes at Station NAP were characterized by the high dominance of a few species and the changes of their ratios in the upper trap with the seasonal changes in the sea-ice concentration. Cannobotryidae (*Amphimelissa setosa* adult and its juvenile forms) was dominant during the open-water season and around the beginning and the end of ice-cover seasons, while Actinommidae (Actinommidae spp. juvenile forms, *Actinomma l. leptodermum*, *Actinomma boreale*) was dominant during the ice-cover season (Fig. 5). These might explain the regional difference in the radiolarian species in the Arctic Ocean. Cannobotryidae was dominant in Arctic marginal sea sediments (Iceland, Barrents, and Chukchi Seas) where sea-ice disappeared in the summer but Actinommidae was dominant in the central Arctic Ocean (Nansen, Amundsen, and Makarov Basins) where the sea surface was covered by sea-ice throughout the year (Bjørklund and Kruglikova, 2003). The summer ice edge accompanies well-grown ice algae, ice fauna (Horner et al., 1992; Michel et al., 2002; Assmy et al., 2013) and favorable alternation between stable water masses and deep vertical mixing where the nutrients are brought to the surface (Harrison and Cota, 1991). Swanberg and Eide (1992) found that abundance of *A. setosa* and its juveniles were correlated well with chlorophyll *a* and phaeopigments along the ice edge in summer in the Greenland Sea. Thus *A. setosa* prefer water masses near the summer ice edge for reproduction and growth.

From the upper trap, a flux peak of *A. setosa* juvenile occurred in the end of sea-ice season, and that of *A. setosa* adult occurred in the beginning of sea-ice season (Fig. 7). The time interval of these peaks might indicate that *A. setosa* have a three months life cycle. *Pseudodictyophimus clevei* also have their flux peaks during the beginning of sea-ice season (November–December) (Fig. 7). These two species seem to prefer to live under cold water mass with sea-ice formation. On the contrary, juvenile stages of Actinommidae were dominant during the ice-cover season (Fig. 5). There-

fore, we interpreted that Actinommidae were tolerant to oligotrophic and stratified cold water masses. Itaki and Bjørklund, 2007 reported that the juvenile stage Actinommids could reproduce as well as adult stage since they found conjoined Actinommidae skeletons from Japan Sea sediments. Furthermore, the flux of Actinommidae spp. juvenile forms increased towards the end of the sea-ice cover season and accompanied with increasing of downward shortwave radiation (Figs. 5 and 7). This might indicate that Actinommidae spp. juvenile forms feeds on algae growing on the ice or other phytoplankton under the sea-ice.

This study showed that the productivity of radiolarian was low but diversity was high under the sea-ice (Figs. 5 and 6). In contrast, radiolarian fauna in the sediment trap set in the Okhotsk Sea showed low diversity during the winter to spring when seasonal sea-ice covered the surface (Okazaki et al., 2003). The maximum total radiolarian flux during the summer season around the sea-ice edge and the open water is characterized by high dominance of *A. setosa* (> 90 %) in our area. Such high dominance of single species does not occur and major nine taxa contributed more than 60 % to the radiolarian assemblage in the Okhotsk Sea (Okazaki et al., 2003). *Amphimelissa setosa*, which have small and delicate siliceous skeleton, might respond to primary production more directly and rapidly and develop earlier than Actinommidae, which have more robust skeleton. Therefore, *Amphimelissa setosa* and Actinommidae have different nutritional niches.

Actinomma boreale, *Spongotrochus glacialis*, *Joergensenium* sp. A were probably related to food supply to the PWW during the sea-ice free season. Relatively higher fluxes of these three species in the upper trap in summer 2012 than in summer 2011 might be due to an effect of the deeper mooring depth of the trap after October 2011 (Figs. 7 and S1). This might be caused by their vertical distribution patterns, as they are more abundant at depths lower than the first upper trap depth (about 180 m) (Fig. 3a). On the other hand, *Ceratocyrtis histricosus* and *Tripodiscium gephyristes* in the upper trap showed increase in their fluxes from May to September in summer 2012. The water temperature at the upper trap depth also increased during the same period (Figs. 7

and S1), we therefore interpreted their increase to be related to the mixing of nutrient and warm upper AW and under PWW, rather than a decrease in sea ice concentrations due to their preference of the warm upper AW.

5.4.2 Radiolarian fauna and between year difference in ocean circulation

Intensification of geostrophic currents on the periphery of Beaufort Gyre (Fig. 1) has been reported in recent years (Nishino et al., 2011; McPhee, 2013). This intensification is caused by increasing volume of water from sea-ice melt associated with the reduction of arctic summer sea-ice and the river runoff to the basins (Proshutinsky et al., 2009; Yamamoto-Kawai et al., 2008). The total radiolarian flux showed lower production during summer (July–September) in 2012 than in 2011 in the both upper and lower traps and especially in the lower trap (Fig. 5). Most of radiolarian taxa also showed lower flux during summer of 2012 (Fig. 7). On the other hand, fluxes of Actinommidae (Actinommidae spp. juvenile forms, *Actinomma l. leptodermum*, *Actinomma boreale*) that might be adapted to the cold and oligotrophic water showed higher values during December 2011–September 2012 than during December 2010–September 2011. Actinommidae spp. juvenile forms and *A. l. leptodermum* were most abundant in the depth interval of 0–100 m at Station 56 in the southwestern Canada Basin. Therefore, we interpreted that cold and oligotrophic water in the Canada Basin began to spread to Station NAP in the Northwind Abyssal Plain from December 2011 and continued to affect the radiolarian fluxes at least until September 2012. McLaughlin et al. (2011) reported that the position of the center of the Beaufort Gyre shifted westwards and that the area under the influence of the gyre spread northwards and westwards in recent years. Moreover, high-resolution pan-Arctic Ocean model results also showed that the Beaufort Gyre expanded with shifting of its center from the Canada Basin interior to the Chukchi Borderland in 2012 compared with 2011, and the ocean current direction in the surface 100 m layer switched northwestward to southwestward in December in 2011 (E. Watanabe, personal communication, 2014). Thus, recent intensification of currents on the Beaufort Gyre associated with sea-ice reduction would have affected

the surface water mass conditions and the biological pump system in the western Arctic Ocean.

5.4.3 Vertical and lateral Transport

Flux peaks of total radiolarians in the lower trap are delayed by about two weeks in comparison to the upper trap (Fig. 5). Therefore, the sinking speed of the aggregated radiolarian particle flux between these depths were averaged to 74 m day^{-1} during November–December 2010, 86 m day^{-1} during July–August 2011, and 73 m day^{-1} during November 2011. Watanabe et al. (2014) simulated movement of cold and warm eddies using a high-resolution pan-Arctic Ocean model, and suggested that the high total mass flux during October–December 2010 at Station NAP, as we determined using sediment samples, was mainly due to the enhancement of the marine biological pump by an anti-cyclonic cold eddy. Shelf-break eddies induce the lateral transport of resuspended bottom sediments composed of old carbon, and enhance the biological pump (O'Brien et al., 2013; Watanabe et al., 2014). Actually, the passage of the cold eddy was observed from a cooling and a deepening of the moored trap depth in the corresponding period (Fig. S1). *Amphimelissa setosa* was the most dominant (> 90 %) during this period and the radiolarian species composition was not changed before and after the cold eddy passage. Therefore the cold eddy in addition to seasonal water mass variations with sea ice formation would enhance the high radiolarian flux, but not diversity, in 2010.

Radiolarian fluxes in the lower trap were generally higher than that in the upper trap except for during May–September in 2012 (Fig. 5). The extremely low fluxes in the lower trap during May–September in 2012 might be due to a decrease of aggregate formation. The aggregate formation, which helps rapid sinking of biogenic particles, would be suppressed by influx of oligotrophic surface water originating from the Beaufort Gyre in the Canada Basin. In the southwestern Canada Basin (Station 56), high standing stock of dead radiolarian specimens (Fig. 2) might indicate an inefficient biological pump in the Canada Basin. In addition, fluxes of Actinommidae spp. juvenile forms were lower in

the lower trap in spite of their high abundance in the upper trap since December 2011. We speculated that the disappearance of fluxes of Actinommidae spp. juvenile forms in the lower trap might be due to lack of aggregate formation.

Higher abundance in the lower trap rather than the upper trap in species having, a wide vertical distribution (*Pseudodictyophimus g. gracilipes*, *Pseudodictyophimus plathycephalus*) or intermediate to deep water distribution (*Ceratocyrtis histricosus, Tripodiscium gephyristes*, Plagiacanthidae gen. et sp. in det., and *Cycladophora davisiana*) might be attributed to the reproduction of these species in a depth between the upper and lower traps. The seasonal changes in the fluxes of intermediate and deep dwellers in the lower trap would reflect the food supply. Flux of deep water dwellers (*Pseudodictyophimus g. gracilipes*, *Pseudodictyophimus plathycephalus*, Plagiacanthidae gen. et sp. in det., *Cycladophora davisiana*) in the lower trap was high during July–August in 2011. This would probably indicate that decomposing material from the primary production during the sea-ice free season was transported to great depths, giving nutrition to the deep water radiolarian fauna. Most of the radiolarian species in the lower trap also peaks during March in 2011, which corresponded to the period with a heavy ice cover and a low downward shortwave radiation. In addition, the flux peak during March in 2011 was made up of more than 80 % of *A. setosa*, which were surface water species although the peaks around the same period were not found in the upper trap. Therefore, the flux peaks during March in 2011 would be derived from some lateral advection at a depth lower than 180 m or a re-suspension of shelf bottom materials into the upper water column.

The Supplement related to this article is available online at doi:10.5194/bgd-11-16645-2014-supplement.

Acknowledgements. We are grateful to the captain, officers and crews of the CCGS *Sir Wilfrid Laurier*, R.V. *Mirai* (JAMSTEC), operated by GODI, R/V, Humfrey Melling (IOS, Canada),

Shigeto Nishino for their help in the mooring operation and sampling collection. We are thankful to A. Matul (P.P. Shirshov Institute of Oceanology, Russian Academy of Sciences, Moscow) for critically reading and commenting on our manuscript. This work was supported by JSPS KAKENHI Grant Number 22221003 to NH and JSPS KAKENHI Grant Number 24•4155 and 26740006 to TI. TI received partial fund from Tatsuro Matsumoto Scholarship Fund of the Kyushu University.

References

Aagaard, K., Coachman, L. K., and Carmack, E.: On the halocline of the Arctic Ocean, Deep-Sea Res. Pt. I, 28, 529–545, 1981.

Aagaard, K., Swift, J. H., and Carmack, E. C.: Thermohaline circulation in the Arctic Mediterranean seas, J. Geophys. Res., 90, 4833–4846, 1985.

Adl, S. M., Simpson, G. B., Farmer, M. A., Andersen, R. A., Anderson, O. R., Barta, J. R., Bowser, S. S., Brugerolle, G., Fensome, R. A., Fredericq, S., James, T. Y., Karpov, S., Kugrens, P., Krug, J., Lane, C. E., Lewis, L. A., Lodge, J., Lynn, D. H., Mann, D. G., Mccourt, R. M., Mendoza, L., Moestrup, Ø., Mozley-Standridge, S. E., Nerad, T. A., Shearer, C. A., Smirnov, A. V., Spiegel, F. W., and Taylor, M. F. J. R.: The new higher level classification of Eukaryotes with emphasis on the taxonomy of protists, J. Eukaryot. Microbiol. 52, 399–451, 2005.

Allen, A. P. and Gilooly, J. F.: Assessing latitudinal gradients in speciation rates and biodiversity at the global scale, Ecol. Lett., 9, 947–954, 2006.

Anderson, O. R.: Radiolaria, Springer, New York, 365 pp., 1983.

Anderson, O. R., Nigrini, C., Boltovskoy, D., Takahashi, K., and Swanberg, N. R.: Class polycystina, in: The Second Illustrated Guide to the Protozoa, edited by: Lee, J. J., Leedale, G. F., and Bradbury, P., Soc. Protozool., Lawrence, KS, 994–1022, 2002.

Arrigo, K. R., Perovich, D. K., Pickart, R. S., Brown, Z. W., van Dijken, G. L., Lowry, K. E., Mills, M. M., Palmer, M. A., Balch, W. M., Bahr, F., Bates, N. R., Benitez-Nelson, C., Bowler, B., Brownlee, E., Ehn, J. K., Frey, K. E., Garley, R., Laney, S. R., Lubelczyk, L., Mathis, J., Matsuoka, A., Mitchell, B. G., Moore, G. W. K., Ortega-Retuerta, E., Pal, S., Polashenski, C. M., Reynolds, R. A., Scheiber, B., Sosik, H. M., Stephens, M., and

Swift, J. H.: Massive phytoplankton blooms under Arctic sea ice, Science, 336, 1408, doi:10.1126/science.1215065, 2012.

Assmy, P., Ehn, J. K., Fernández-Méndez, M., Hop, H., Katlein, C., Sundfjord, A., Bluhm, K., Daase, M., Engel, A., Fransson, A., Granskog, M. A., Hudson, S. R., Kristiansen, S., Nicolaus, M., Peeken, I., Renner, A. H. H., Spreen, G., Tatarek, A., and Wiktor, J.: Floating ice–algal aggregates below melting Arctic Sea ice, PLoS ONE, 8, e76599, doi:10.1371/journal.pone.0076599, 2013.

Bailey, J. W.: Notice of microscopic forms found in the soundings of the Sea of Kamtschatka, Am. J. Sci. Arts, 22, 1–6, 1856.

Bates, N. R. and Mathis, J. T.: The Arctic Ocean marine carbon cycle: evaluation of air-sea CO_2 exchanges, ocean acidification impacts and potential feedbacks, Biogeosciences, 6, 2433–2459, doi:10.5194/bg-6-2433-2009, 2009.

Bates, N. R., Moran, S. B., Hansell, D. A., and Mathis, J. T.: An increasing CO_2 sink in the Arctic Ocean due to sea-ice loss, Geophys. Res. Lett., 33, L23609, doi:10.1029/2006GL027028, 2006.

Bernstein, T.: Zooplankton des Nordlischen teiles des Karischen Meeres, Transactions of the Arctic Institute, IX, 3–58, 1934 (in Russian with German summary).

Bjørklund, K. R. and Kruglikova, S. B.: Polycystine radiolarians in surface sediments in the Arctic Ocean basins and marginal seas, Mar. Micropaleontol., 49, 231–273, 2003.

Bjørklund, K. R., Cortese, G., Swanberg, N., and Schrader, H. J.: Radiolarian faunal provinces in surface sediments of the Greenland, Iceland and Norwegian (GIN) seas, Mar. Micropaleontol., 35, 105–140, 1998.

Bjørklund, K. R., Kruglikova, S. B., and Anderson, O. R.: Modern incursions of tropical Radiolaria into the Arctic Ocean, J. Micropalaeontol., 31, 139–158, doi:10.1144/0262-821X11-030, 2012.

Bjørklund, K. R., Itaki, T., and Dolven, J. K.: Per Theodor Cleve: a short résumé and his radiolarian results from the Swedish Expedition to Spitsbergen in 1898, J. Micropalaeontol., 33, 59–93, 2014.

Boetius, A., Albrecht, S., Bakker, K. B., Bienhold, C., Felden, J., Fernández-Méndez, M., Hendricks, S., Katlein, C., Lalande, C., Krumpen, T., Nicolaus, M., Peeken, I., Rabe, B., Rogacheva, A., Rybakova, E., Somavilla, R., and Wenzhöfer, F.: Export of algal biomass from the melting arctic sea ice, Science, 339, 1430–1432, doi:10.1126/science.1231346, 2013.

Boltovskoy, D., Kling, S. A., Takahashi, K., and Bjørklund, K. R.: World atlas of distribution of recent polycystina (Radiolaria), Palaeontol. Electron., 13, 1–230, available at: http://palaeo-electronica.org/2010_3/215/index.html (last access: 29 November 2014), 2010.
Burridge, A. K., Bjørklund, K. R., Kruglikova, S. B., and Hammer, Ø.: Inter- and intraspecific morphological variation of four-shelled *Actinomma* taxa (Radiolaria) in polar and subpolar regions, Mar. Micropaleontol., 110, 50–71, 2013.
Calbet, A. and Landry, M. R.: Phytoplankton growth, microzooplankton grazing, and carbon cycling in marine systems, Limnol. Oceanogr., 49, 51–57, 2004.
Cavalier-Smith, T. and Chao, E. E. Y.: Phylogeny and classification of phylum Cercozoa (Protozoa), Protist, 154, 341–358, 2003.
Cleve, P. T.: Plankton collected by the Swedish Expedition to Spitzbergen in 1898, Kgl. Svenska Vetensk. Akad. Hand., 32, 1–51, 1899.
Coachman, L. and Barnes, C. A.: The contribution of Bering Sea water to the Arctic Ocean, Arctic, 14, 147–161, 1961.
Coachman, L. K., Aagaard, K., and Tripp, R. B.: Bering Strait: the regional physical oceanography, University of Washington Press, Seattle, 172 pp., 1975.
Comiso, J. C., Parkinson, C. L., Gersten, R., and Stock, L.: Accelerated decline in the Arctic sea ice cover, Geophys. Res. Lett., 35, L01703, doi:10.1029/2007GL031972, 2008.
Cortese, G. and Bjørklund, K. R.: The morphometric variation of *Actinomma boreale* (Radiolaria) in Atlantic boreal waters, Mar. Micropaleontol., 29, 271–282, 1997.
Cortese, G. and Bjørklund, K. R.: The taxonomy of boreal Atlantic Ocean. Actinommida (Radiolaria), Micropaleontology, 44, 149–160, 1998.
Cortese, G., Bjørklund, K. R., and Dolven, J. K.: Polycystine radiolarians in the Greenland–Iceland–Norwegian seas: species and assemblage distribution, Sarsia: North Atlantic Marine Science, 88, 65–88, 2003.
Dolven, J. K., Bjørklund, K. R., and Itaki, T.: Jørgensen's polycystine radiolarian slide collection and new species, J. Micropalaeontol., 33, 21–58, 2014.
Dumitrica, P.: Cleveiplegma n. gen., a new generic name for the radiolarian species Rhizoplegma boreale (Cleve, 1899), Revue de Micropaléontologie, 56, 21–25, 2013.
Ehrenberg, C. G.: Über die Bildung der Kreidefelsen und des Kreidemergels durch unsichtbare Organismen, Abhandlungen, Jahre 1838, K. Preuss. Akad. Wiss., Berlin, 59–147, 1838.
Ehrenberg, C. G.: Über das organischen Leben des Meeresgrundes in bis 10 800 und 12 000 Fuss Tiefe, Bericht, Jahre 1854, K. Preuss. Akad. Wiss., Berlin, 54–75, 1854.

Ehrenberg, C. G.: Über die Tiefgrund-Verhältnisse des Oceans am Eingange der Davisstrasse und bei Island, Monatsberichte. Jahre 1861, K. Preuss. Akad. Wiss., Berlin, 275–315, 1862.
Ehrenberg, C. G.: Mikrogeologischen Studien über das kleinste Leben der Meeres-Tiefgrunde aller Zonen und dessen geologischen Einfluss, Abhandlungen, Jahre 1873, K. Preuss. Akad. Wiss., Berlin, 131–399, 1873.
Ehrenberg, C. G.: Fortsetzung der mikrogeologischen Studien als Gesammt-Uebersicht der mikroskopischen Palaontologie gleichartig analysirter Gebirgsarten der Erde, mit specieller Rucksicht auf den Polycystinen-Mergel von Barbados, Abhandlungen, Jahre 1875, K. Preuss. Akad. Wiss., Berlin, 1–225, 1875.
Ewing, M. and Connary, S.: Nepheloid layer in the North Pacific, in: Geological Investigations of the North Pacific, edited by: Hays, J. D., Geol. Soc. Am. Mem., 126, 41–82, 1970.
Francois, R., Honjo, S., Krishfield, R., and Manganini, S.: Factors controlling the flux of organic carbon to the bathypelagic zone of the ocean, Global Biogeochem. Cy., 16, 1087, doi:10.1029/2001GB001722, 2002.
Haeckel, E.: Die Radiolarien (Rhizopoda Radiaria) – Eine Monographie, Reimer, Berlin, 572 pp., 1862.
Haeckel, E.: Über die Phaeodarien, eine neue Gruppe kieselschaliger mariner Rhizopoden, Jenaische Zeitschrift für Naturwissenschaft, 14, 151–157, 1879.
Haeckel, E.: Prodromus Systematis Radiolarium, Entwurf eines Radiolarien-Systems auf Grund von Studien der Challenger-Radiolarien, Jenaische Zeitschrift für Naturwissenschaft, 15, 418–472, 1881.
Haeckel, E.: Report on the Radiolaria collected by the H.M.S. *Challenger* during the Years 1873–1876, Report on the Scientific Results of the Voyage of the H.M.S. *Challenger*, Zoology, 18, 1–1803, 1887.
Harrison, W. G. and Cota, G. F.: Primary production in polar waters: relation to nutrient availability, Polar Res., 10, 87–104, 1991.
Hertwig, R.: Der Organismus der Radiolarien, Jenaische Denkshr., 2, 129–277, 1879.
Honjo, S., Krishfield, R. A., Eglinton, T. I., Manganini, S. J., Kemp, J. N., Doherty, K., Hwang, J., Mckee, T. K., and Takizawa, T.: Biological pump processes in the cryopelagic and hemipelagic Arctic Ocean: Canada Basin and Chukchi Rise, Prog. Oceanogr., 85, 137–170, 2010.

Horner, R. A., Ackley, S. F., Dieckmann, G. S., Gulliksen, B., Hoshiai, T., Legendre, L., Melnikov, I. A., Reeburgh, W. S., Spindler, M., and Sullivan, C. W.: Ecology of sea ice biota. 1. Habitat, terminology, and methodology, Polar Biol., 12, 417–427, 1992.

Hülseman, K.: Radiolaria in plankton from the Arctic drifting station T-3, including the description of three new species, Arc. Inst. North Am. Tech. Pap., 13, 1–52, 1963.

Ikenoue, T., Ishitani, Y., Takahashi, K., and Tanaka, S.: Seasonal flux changes of radiolarians at Station K2 in the Western Subarctic Gyre, Umi no Kenkyu (Oceanography in Japan), 19, 165–185, 2010 (in Japanese, with English abstract).

Ikenoue, T., Takahashi, K., and Tanaka, S.: Fifteen year time-series of radiolarian fluxes and environmental conditions in the Bering Sea and the central subarctic Pacific, 1990–2005, Deep-Sea Res. Pt. II, 61–64, 17–49, 2012a.

Ikenoue, T., Ueno, H., and Takahashi, K.: Rhizoplegma boreale (Radiolaria): a tracer for mesoscale eddies from coastal areas, J. Geophys. Res., 117, C04001, doi:10.1029/2011JC007728, 2012b.

Ishitani, Y. and Takahashi, K.: The vertical distribution of Radiolaria in the waters surrounding Japan, Mar. Micropaleontol., 65, 113–136, 2007.

Ishitani, Y., Takahashi, K., Okazaki, Y., and Tanaka, S.: Vertical and geographic distribution of selected radiolarian species in the North Pacific, Micropaleontology, 54, 27–39, 2008.

Itaki, T. and Bjørklund, K. R.: Conjoined radiolarian skeletons (Actinommidae) from the Japan Sea sediments, Micropaleontology, 53, 371–389, 2007.

Itaki, T., Ito, M., Narita, H., Ahagon, M., and Sakai, I.: Depth distribution of radiolarians from the Chukchi and Beaufort Seas, western Arctic, Deep-Sea Res. Pt. I, 50, 1507–1522, 2003.

Itoh, M., Nishino, S., Kawaguchi, Y., and Kikuchi, T.: Barrow Canyon fluxes of volume, heat and freshwater revealed by mooring observations, J. Geophys. Res., 118, 4363–4379, 2013.

Jackson, J. M., Allen, S. E., McLaughlin, F. A., Woodgate, R. A., and Carmack, E. C.: Changes to the near surface waters in the Canada Basin, Arctic Ocean from 1993–2009: a basin in transition, J. Geophys. Res., 116, C10008, doi:10.1029/2011JC007069, 2011.

Jones, E. P. and Anderson, L. G.: On the origin of the chemical properties of the Arctic Ocean halocline, J. Geophys. Res., 91, 10759–10767, 1986.

Jørgensen, E.: Protophyten und Protozöen im Plankton aus der norwegischen Westküste, Bergens Museumus Aarbog 1899, 6, 51–112, 1900.

Jørgensen, E.: The Protist plankton and the diatoms in bottom samples, Plates VIII–XVIII, Bergens Museuns Skrifter, 1, 49–151, 1905.

Kling, S. A.: Vertical distribution of polycystine radiolarians in the central North Pacific, Mar. Micropaleontol., 4, 295–318, 1979.

Kozur, H. and Möstler, H.: *Entactinaria subordo* Nov., a new radiolarian suborder, Geologisch Paläontologische Mitteilungen, Innsbruck, 11, 399–414, 1982.

Kruglikova, S. B.: Distribution of Polycystine radiolarians from recent and Pleistocene sediments of the Arctic-boreal zone, Berichte zur Polarforschung (Reports on Polar Research), 306, 120–133, 1999.

Kruglikova, S. B., Bjørklund, K. R., Hammer, Ø., and Anderson, O. R.: Endemism and speciation in the polycystine radiolarian genus *Actinomma* in the Arctic Ocean: description of two new species *Actinomma georgii* n. sp., and *A. turidae* n. sp., Mar. Micropaleontol., 72, 26–48, 2009.

Kruglikova, S. B., Bjørklund, K. R., Dolven, J. K., Hammer, Ø., and Cortese, G.: High-rank polycystine radiolarian taxa as temperature proxies in the Nordic Seas, Stratigraphy, 7, 265–281, 2010.

Kruglikova, S. B., Bjørklund, K. R., and Hammer, O.: High rank taxa of Polycystina (Radiolaria) as environmental bioindicators, Micropaleontology, 57, 483–489, 2011.

Markus, T., Stroeve, J. C., and Miller, J.: Recent changes in Arctic sea ice melt onset, freezeup, and melt season length, J. Geophys. Res., 114, C12024, doi:10.1029/2009JC005436, 2009.

Matul, A. and Abelmann, A.: Pleistocene and Holocene distribution of the radiolarian *Amphimelissa setosa* Cleve in the North Pacific and North Atlantic: evidence for water mass movement, Deep-Sea Res. Pt. II, 52, 2351–2364, 2005.

McLaughlin, F. A., Carmack, E., Proshutinsky, A., Krishfield, R. A., Guay, C. K., Yamamoto-Kawai, M., Jackson, J. M., and Williams, W. J.: The rapid response of the Canada Basin to climate forcing: From bellwether to alarm bells, Oceanography, 24, 146–159, doi:10.5670/oceanog.2011.66, 2011.

McPhee, M.: Intensification of geostrophic currents in the Canada Basin, Arctic Ocean, J. Climate, 26, 3130, doi:10.1175/JCLI-D-12-00289.1, 2013.

Michel, C., Nielsen, T. C., Nozais, C., and Gosselin, M.: Significance of sedimentation and grazing by ice micro- and meiofauna for carbon cycling in annual sea ice (northern Baffin Bay), Aquat. Microb. Ecol., 30, 57–68, 2002.

Murray, J.: The Radiolaria. Narrative of the cruise of the H.M.S. "*Challenger*" with a general account of the scientific results of the expedition, in: Report from the Voyage of the H.M.S.

Challenger, edited by: Tizard, T. H., Moseley, H. N., Buchanan, J. Y., and Murray, J., Narrative, 1, 219–227, 1885.

Müller, J.: Über die Thalassicollen, Polycystinen und Acanthometren des Mittelmeeres, Abhandlungen, Jahre 1858, K. Preuss. Akad. Wiss., Berlin, 1–62, 1858.

Nikolaev, S. I., Berney, C., Fahrni, J., Bolivar, I., Polet, S., Mylnikov, A. P., Aleshin, V. V., Petrov, N. B., and Pawlowski, J.: The twilight of Heliozoa and rise of Rhizaria, an emerging supergroup of amoeboid eukaryotes, P. Natl. Acad. Sci. USA, 101, 8066–8071, 2004.

Nimmergut, A. and Abelmann, A.: Spatial and seasonal changes of radiolarian standing stocks in the Sea of Okhotsk, Deep-Sea Res. Pt. I, 49, 463–493, 2002.

Nishino, S., Kikuchi, T., Yamamoto-Kawai, M., Kawaguchi, Y., Hirawake, T., and Itoh, M.: Enhancement/reduction of biological pump depends on ocean circulation in the sea-ice reduction regions of the Arctic Ocean, J. Oceanogr., 67, 305–314, doi:10.1007/s10872-011-0030-7, 2011.

Nishino, S.: R/V *Mirai* cruise report MR13-06, ,226 pp., available at: www.godac.jamstec.go.jp/darwin/datatree/e (last access: 29 November 2014), JAMSTEC, Yokosuka, Japan, 2013.

NSIDC (National Snow and Ice Data Center): Arctic sea ice extent settles at record seasonal minimum, available at: http://nsidc.org/arcticseaicenews/2012/09/ (last access: 29 November 2014), 2012.

O'Brien, M. C., Melling, H., Pedersen, T. F., and Macdonald, R. W.: The role of eddies on particle flux in the Canada Basin of the Arctic Ocean, Deep-Sea Res. Pt. I, 71, 1–20, 2013.

Okazaki, Y., Takahashi, K., Yoshitani, H., Nakatsuka, T., Ikehara, M., and Wakatsuchi, M.: Radiolarians under the seasonally sea-ice covered conditions in the Okhotsk Sea: flux and their implications for paleoceanography, Mar. Micropaleontol., 49, 195–230, 2003.

Okazaki, Y., Takahashi, K., Itaki, T., and Kawasaki, Y.: Comparison of radiolarian vertical distributions in the Okhotsk Sea near the Kuril Islands and in the northwestern North Pacific off Hokkaido Island, Mar. Micropaleontol., 51, 257–284, 2004.

Okazaki, Y., Takahashi, K., Onodera, J., and Honda, M. C.: Temporal and spatial flux changes of radiolarians in the northwestern Pacific Ocean during 1997–2000, Deep-Sea Res. Pt. II, 52, 2240–2274, 2005.

Petrushevskaya, M. G.: Radiolarians of orders Spumellaria and Nassellaria of the Antarctic region (from material of the Soviet Antarctic Expedition), in: Studies of Marine Fauna IV(XII): Biological Reports of the Soviet Antarctic Expedition (1955–1958), edited by: Andriyashev, A. P. and Ushakov, P. V., Academy of Sciences of the USSR, Zoological Institute, Leningrad, 3,

2–186, 1967 (translated from Russian and published by Israel Program for Scientific Translations, 1968).

Petrushevskaya, M. G.: Radiolyarii Nassellaria v planktone Mirovogo Okeana, Issledovaniya Fauny Morei, 9, 1–294, 1971 (+ App., 374–397), Nauka, Leningrad, in Russian.

Popofsky, A.: Die Radiolarien der Antarktis (mit Ausnahme der Tripyleen), in: Deutsche Südpolar-Expedition 1901–1903. X, Zoologie, 2, part 3, edited by: Drygalski, E., Georg Reimer, Berlin, 184–305, 1908.

Proshutinsky, A., Bourke, R. H., and McLaughlin, F. A.: The role of the Beaufort Gyre in Arctic climate variability: seasonal to decadal climate scales, Geophys. Res. Lett., 29, 2100, doi:10.1029/2002GL015847, 2002.

Proshutinsky, A., Krishfield, R., Timmermans, M. L., Toole, J., Carmack, E., McLaughlin, F., Williams, W. J., Zimmermann, S., Itoh, M., and Shimada, K.: Beaufort Gyre freshwater reservoir: state and variability from observations, J. Geophys. Res., 114, C00A10, doi:10.1029/2008JC005104, 2009.

Reynolds, R. W., Rayner, N. A., Smith, T. M., Stokes, D. C., and Wang, W.: An improved in situ and satellite SST analysis for climate, J. Climate, 15, 1609–1625, 2002.

Riedel, W. R.: Subclass radiolaria, in: The Fossil Record, edited by: Harland, W. B. et al., Geol. Soc. London, London, UK, 291–298, 1967.

Saha, S., Moorthi, S., Pan, H. L., Wu, X. R., Wang, J. D., Nadiga, S., Tripp, P., Kistler, R., Woollen, J., Behringer, D., Liu, H. X., Stokes, D., Grumbine, R., Gayno, G., Wang, J., Hou, Y. T., Chuang, H. Y., Juang, H. M. H., Sela, J., Iredell, M., Treadon, R., Kleist, D., Van Delst, P., Keyser, D., Derber, J., Ek, M., Meng, J., Wei, H. L., Yang, R. Q., Lord, S., Van den Dool, H., Kumar, A., Wang, W. Q., Long, C., Chelliah, M., Xue, Y., Huang, B. Y., Schemm, J. K., Ebisuzaki, W., Lin, R., Xie, P. P., Chen, M. Y., Zhou, S. T., Higgins, W., Zou, C. Z., Liu, Q. H., Chen, Y., Han, Y., Cucurull, L., Reynolds, R. W., Rutledge, G., and Goldberg, M.: The NCEP climate forecast system reanalysis, B. Am. Meteorol. Soc., 91, 1015–1057, 2010.

Samtleben, C., Schäfer, P., Andruleit, H., Baumann, A., Baumann, K. H., Kohly, A., Matthiessen, J., and Schröder-Ritzrau, A.: Plankton in the Norwegian–Greenland Sea: from living communities to sediment assemblages – an actualistic approach, Geol. Rundsch., 84, 108–136, 1995.

Shannon, C. E. and Weaver, W.: The Mathematical Theory of Communication, University of Illinois Press, Urbana, 125 pp., 1949.

Shimada, K., Carmack, E. C., Hatakeyama, K., and Takizawa, T.: Varieties of shallow temperature maximum waters in the western Canadian Basin of the Arctic Ocean, Geophys. Res. Lett., 28, 3441–3444, 2001.

Shimada, K., Kamoshida, T., Itoh, M., Nishino, S., Carmack, E., McLaughlin, F., Zimmermann, S., and Proshutinsky, A.: Pacific Ocean inflow: influence on catastrophic reduction of sea ice cover in the Arctic Ocean, Geophys. Res. Lett., 33, L08605, doi:10.1029/2005GL025624, 2006.

Stroeve, J., Holland, M. M., Meier, W., Scambos, T., and Serreze, M.: Arctic sea ice decline: faster than forecast, Geophys. Res. Lett., 34, L09501, doi:10.1029/2007GL029703, 2007.

Stroeve, J. C., Serreze, M. C., Holland, M. M., Kay, J. E., Malanik, J., and Barrett, A. P.: The Arctic's rapidly shrinking sea ice cover: a research synthesis, Climatic Change, 110, 1005–1027, doi:10.1007/s10584-011-0101-1, 2012.

Swanberg, N. R. and Eide, L. K.: The radiolarian fauna at the ice edge in the Greenland Sea during summer, 1988, J. Mar. Res., 50, 297–320, 1992.

Takahashi, K.: Radiolaria: flux, ecology, and taxonomy in the Pacific and Atlantic, in:, Ocean Biocoenosis, Ser. 3, edited by: Honjo, S., Woods Hole Oceanographic Institution Press, Woods Hole, MA, 303 pp., 1991.

Takahashi, K. and Anderson, O. R.: Class Phaeodaria, in: The Second Illustrated Guide to the Protozoa, edited by: Lee, J. J., Leedale, G. F., and Bradbury, P., Soc. Protozool., Lawrence, KS, 981–994, 2002.

Takahashi, K. and Honjo, S.: Vertical flux of Radiolaria: a taxon-quantitative sediment trap study from the western tropical Atlantic, Micropaleontology, 27, 140–190, 1981.

Tibbs, J. F.: On some planktonic Protozoa taken from the track of Drift Station Arlis I, 1960–1961, J. Arct. Inst. N. Am., 20, 247–254, 1967.

Watanabe, E., Onodera, J., Harada, N., Honda, M. C., Kimoto, K., Kikuchi, T., Nishino, S., Matsuno, K., Yamaguchi, A., Ishida, A., and Kishi, M. J.: Enhanced role of eddies in the Arctic marine biological pump, Nat. Commun., 5, 3950, doi:10.1038/ncomms4950, 2014.

Welling, L. A.: Environmental control of radiolarian abundance in the central equatorial Pacific and implications for paleoceanographic reconstructions, Ph.D. thesis, Oregon State Univ., Corvallis, 314 pp., 1996.

Yamamoto-Kawai, M., McLaughlin, F. A., Carmack, E. C., Nishino, S., and Shimada, K.: Freshwater budget of the Canada Basin, Arctic Ocean, from salinity, δ^{18}O, and nutrients, J. Geophys. Res., 113, C01007, doi:10.1029/2006JC003858, 2008.

Yang, J.: Seasonal and interannual variability of downwelling in the Beaufort Sea, J. Geophys. Res., 114, C00A14, doi:10.1029/2008JC005084, 2009.

Yuasa, T., Takahashi, O., Honda, D., and Mayama, S.: Phylogenetic analyses of the polycystine Radiolaria based on the 18s rDNA sequences of the Spumellarida and the Nassellarida, Eur. J. Protistol., 41, 287–298, 2005.

Table 1. Logistic and sample information for the vertical plankton tows for radiolarian standing stock (S. S.) at two stations during R/V *Mirai* Cruise MR13-06.

Station ID		Sampling time (UTC)	Depth interval (m)	Flow water mass (m^3)	Aliquot size	Living radiolarian S.S. (count)	Dead radiolarian S.S. (count)	Total radiolarian S.S. (count)
Station 32	74°32′ N, 161°54′ W	01:24	0–100	20.4	1/4	247 (1257)	75 (381)	322 (1638)
		01:22	100–250	27.2	1/4	96 (654)	116 (790)	212 (1444)
Date	9 Sep 2013	01:18	250–500	39.7	1/2	11 (215)	20 (397)	31 (612)
		01:10	500–1000	79.3	1/2	12 (462)	17 (665)	29 (1127)
Station 56	73°48′ N, 159°59′ W	17:36	0–100	15.8	1/4	499 (1968)	677 (2671)	1176 (4639)
		17:34	100–250	23.8	1/2	265 (3156)	480 (5711)	745 (8867)
Date	27 Sep 2013	17:30	250–500	40.8	1/2	55 (1125)	276 (5627)	331 (6752)
		17:22	500–1000	81.8	1/2	25 (1034)	83 (3381)	108 (4415)

Table 2. Locations, mooring depths, standard sampling interval, and sampled duration of sediment trap station in the western Arctic Ocean.

Trap station	Latitude	Longitude	Water depth (m)	Mooring depth (m)	Standard sampling interval* (days)	Sampled duration
NAP10t	75°00′ N	162°00′ W	1975	184 (upper), 1300 (lower)	10–15	4 Oct 2010–28 Sep 2011
NAP11t	75°00′ N	162°00′ W	1975	260 (upper), 1360 (lower)	10–15	4 Oct 2011–18 Sep 2012

* Details of the exact durations for each sample are shown in Tables S3 and S4.

Table 3. List of 51 radiolarian taxa encountered in the plankton tow and sediment trap samples.

	References
Radiolaria, Müller (1858)	
Polycystina, Ehrenberg (1838); emend. Riedel (1967)	
Spumellaria, Ehrenberg (1875)	
Actinommidae, Haeckel (1862); emend. Riedel (1967)	
Actinomma boreale, Cleve (1899)	Cortese and Bjørklund (1998), Plate 1, Figs. 1–18
Actinomma leptodermum leptodermum, Jørgensen (1900)	Cortese and Bjørklund (1998), Plate 2, Figs. 1–14
Actinomma morphogroup A	
Actinomma leptodermum, Jørgensen (1900); *longispinum*, Cortese and Bjørklund (1998)	Cortese and Bjørklund (1998), Plate 2, Figs. 15–22
Actinomma leptodermum longispinum juvenile	
Actinommidae spp. juvenile forms	
Actinomma turidae, Kruglikova and Bjørklund (2009)	Kruglikova et al. (2009), Plate 5, Figs. 1–35, Plate 6, Figs. 1–28
Actinomma morphogroup B	
Actinomma morphogroup B juvenile	
**Drymyomma elegans*, Jørgensen (1900)	Dolven et al. (2014), Plate 1, Figs. 5–7
**Actinomma friedrichdreyeri*, Burridge, Bjørklund and Kruglikova (2013)	Burridge et al. (2013), Plate 6, Figs. 7–15, Plate 7, Figs. 3–15
Arachnosphaera dichotoma, Jørgensen (1900)	Dolven et al. (2014), Plate 1, Figs. 1–4
Litheliidae, Haeckel (1862)	
* *Streblacantha circumtexta*? Jørgensen (1905)	
Spongodiscidae, Haeckel (1862)	
Spongotrochus glacialis, Popofsky (1908)	Bjørklund et al. (1998), Plate I, Fig. 3
Stylodictya sp.	
Entactinaria, Kozur and Mostler (1982)	
Cleveiplegma boreale, Cleve (1899)	Dumitrica (2013), Plate 1, Figs. 1–9
Joergensenium sp. A	
Joergensenium sp. B	
Nassellaria, Ehrenberg (1875)	
Sethophormididae, Haeckel (1881); emend. Petrushevskaya (1971)	
Enneaphormis rotula, Haeckel (1881)	Petrushevskaya (1971), Fig. 31, I–III
Enneaphormis enneastrum, Haeckel (1887)	Petrushevskaya (1971), Fig. 32, IV, V
Protoscenium simplex, Cleve (1899)	Bjørklund et al. (2014), Plate 9, Figs. 15–17
Plagiacanthidae, Hertwig (1879); emend. Petrushevskaya (1971)	
**Arachnocorys umbellifera*, Haeckel (1862)	Welling (1996), Plate 14, Figs. 24–27
Ceratocyrtis histricosus, Jørgensen (1905)	Petrushevskaya (1971), Figs. 52, II–IV
Ceratocyrtis galeus, Cleve (1899)	Bjørklund et al. (2014), Plate 8, Figs. 1–2
**Cladoscenium tricolpium*, Haeckel (1887)	Bjørklund (1976), Plate 7, Figs. 5–8
Cladoscenium tricolpium?	
Lophophaena clevei, Petrushevskaya (1971)	Petrushevskaya (1971), Fig. 57, I
Phormacantha hystrix, Jørgensen (1900)	Dolven et al. (2014), Plate 6, Figs. 20–24
**Peridium longispinum*? Jørgensen (1900)	Bjørklund et al. (1998), Plate II, Figs. 26 and 27
Plectacantha oikiskos, Jørgensen (1905)	Dolven et al. (2014), Plate 7, Figs. 7–9
Pseudodictyophimus clevei, Jørgensen (1900)	Bjørklund et al. (2014), Plate 9, Figs. 5–7
Pseudodictyophimus gracilipes gracilipes, Bailey (1856)	Bjørklund et al. (1998), Plate II, Figs. 7 and 8
Pseudodictyophimus spp. juvenile forms	
Pseudiodictyophimus gracilipes, Bailey (1856); *bicornis*, Ehrenberg (1861)	Bjørklund and Kruglikova (2003), Plate V, Figs. 16–19
Pseudodictyophimus gracilipes, Bailey (1856); *multispinus*, Bernstein (1934)	Bjørklund and Kruglikova (2003), Plate V, Figs. 11–13
Pseudodictyophimus plathycephalus, Haeckel (1887)	Bjørklund and Kruglikova (2003), Plate V, Figs. 1–5
Tetraplecta pinigera, Haeckel (1887)	Takahashi (1991), Plate. 24, Figs. 1–5
Tripodiscium gephyristes, Hülsemann (1963)	Bjørklund et al. (1998), Plate II, Figs. 20 and 21
Plagiacanthidae gen. et sp. in det.	

Table 3. Continued.

	References
Eucyrtidiidae, Ehrenberg (1847); emend. Petrushevskaya (1971)	
Artostrobus annulatus, Bailey (1856)	Bjørklund et al. (2014), Plate 9, Figs. 1–4
Artostrobus joergenseni, Petrushevskaya (1967)	Petrushevskaya (1971), Fig. 92, VIII–IX
**Cornutella stylophaena*, Ehrenberg (1854)	Petrushevskaya (1967), Fig. 59, I–III
**Cornutella longiseta*, Ehrenberg (1854)	Petrushevskaya (1967), Fig. 62, I–II, Fig. 58, VIII
Cycladophora davisiana, Ehrenberg (1862)	Bjørklund et al. (1998), Plate II, Figs. 1 and 6
Lithocampe platycephala, Ehrenberg (1873)	Bjørklund et al. (1998), Plate II, Figs. 23–25
Lithocampe aff. furcaspiculata, Popofsky (1908)	Petrushevskaya (1967), Fig. 74, I–IV
Sethoconus tabulatus, Ehrenberg (1873)	Bjørklund et al. (2014), Plate 9, Figs. 10 and 11
Cannobotryidae, Haeckel (1881); emend. Riedel (1967)	
Amphimelissa setosa, Cleve (1899)	Bjørklund et al. (1998), Plate II, Figs. 30–33
Amphimelissa setosa, juvenile	
Phaeodaria, Haeckel (1879)	
Lirella melo, Cleve (1899)	Bjørklund et al. (2014), Plate 11, Figs. 5 and 6
Protocystis harstoni, Murray (1885)	Takahashi and Honjo (1981), Plate 11, Fig. 11

All taxa are found in the trap, and * refer to taxa found in trap only.

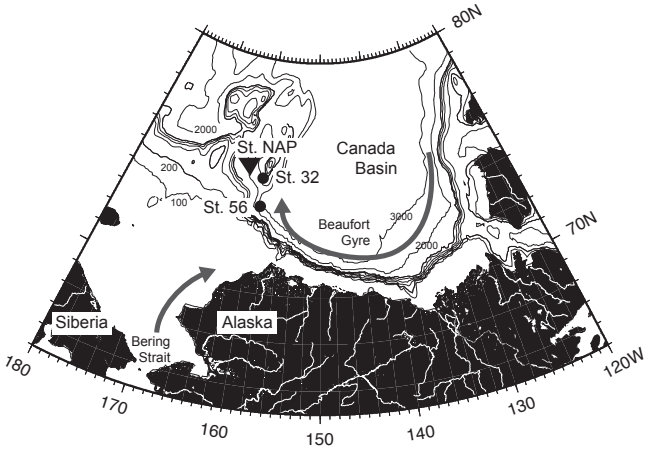

Figure 1. Map of the Chukchi and Beaufort Seas showing the locations of sediment trap (solid triangle) and plankton tows (solid circles). Gray arrows indicate the cyclonic circulation of the Beaufort Gyre and the inflow of Pacific water through the Bering Strait, respectively.

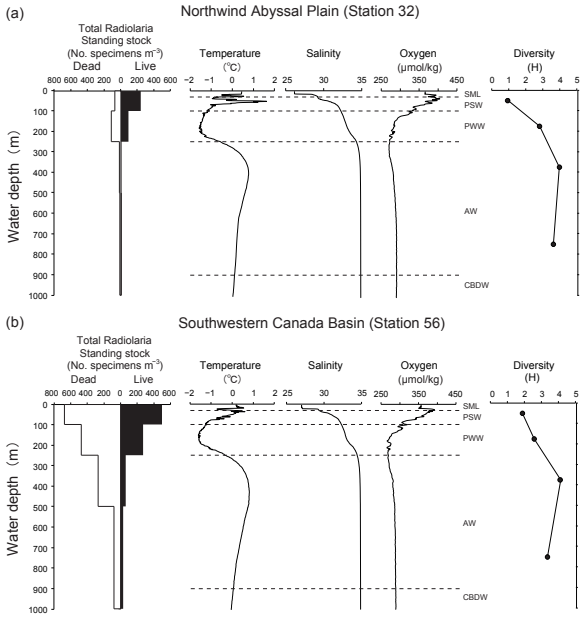

Figure 2. The depth distributions of total dead and living radiolarians at stations 32 **(a)**, and 56 **(b)** in comparison to vertical profiles of temperature, salinity, dissolved oxygen (Nishino, 2013), and living radiolarian diversity index (Shannon and Weaver, 1949). Also the different water masses are identified Surface Mixed Layer (SML), Pacific Summer Water (PSW), Pacific Winter Water (PWW), Atlantic Water (AW), and Canada Basin Deep Water (CBDW).

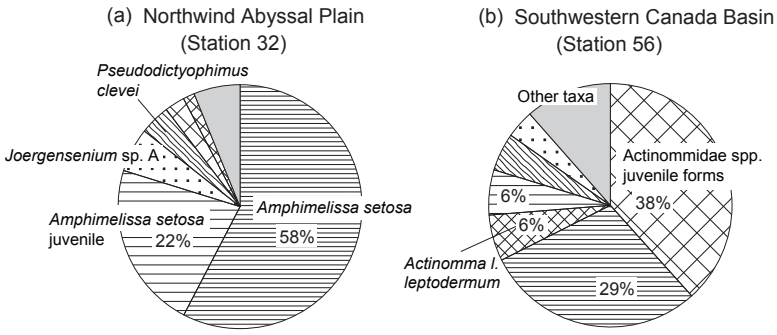

Figure 3. Compositions of living radiolarian assemblages in plankton samples through the upper 1000 m of the water columns at stations 32 (Northwind Abyssal Plain) **(a)** and 56 (southwestern Canada basin) **(b)**.

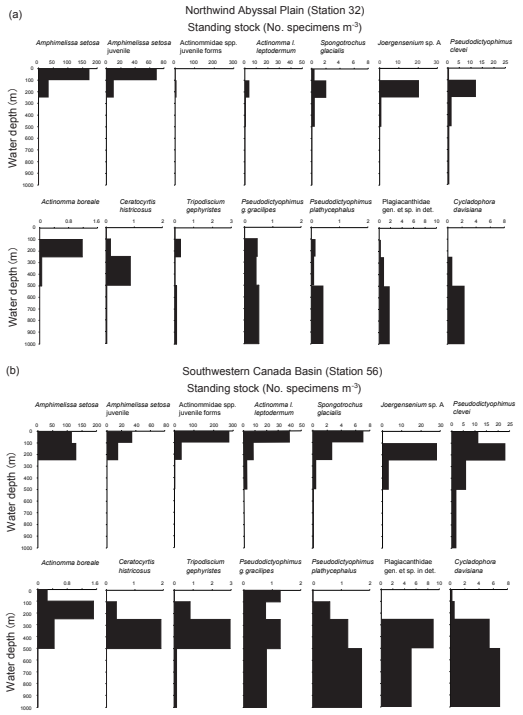

Figure 4. The depth distributions of fourteen living radiolarians in plankton samples at stations 32 **(a)** and 56 **(b)**.

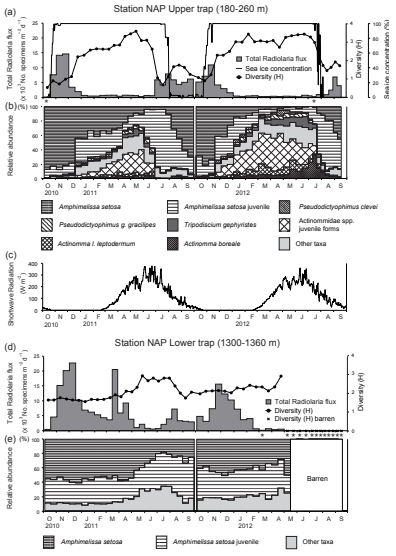

Figure 5. (a) Total radiolarian fluxes with diversity index and sea-ice concentration in upper trap at Station NAP. 2 samples with fewer than 100 specimens are marked with asterisk. Sea-ice concentration data are from Reynolds et al. (2002) (http://iridl.ldeo.columbia.edu/SOURCES/.IGOSS/.nmc/.Reyn_SmithOIv2/). **(b)** Radiolarian faunal compositions in upper trap at Station NAP. **(c)** Downward short wave radiation at the surface of sea-ice and ocean (after sea-ice opening) around Station NAP from National Centers for Environmental Prediction-Climate Forecast System Reanalysis (NCEP-CFSR) (Saha et al., 2010). **(d)** Total radiolarian fluxes with the Shannon–Weaver diversity index in the lower trap at Station NAP. 13 samples with fewer than 100 specimens are marked with asterisk. **(e)** Radiolarian faunal compositions in lower trap at Station NAP. Barren area, no samples due to trap failure.

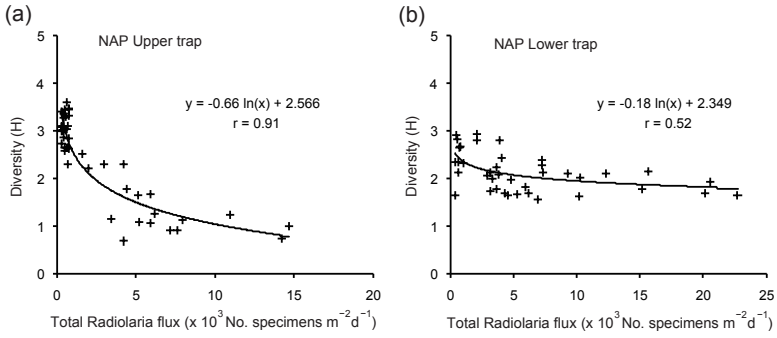

Figure 6. Scatter plots of diversity indices and total radiolarian fluxes at upper **(a)** and lower trap **(b)**. In these plots, samples with fewer than 100 specimens were excluded.

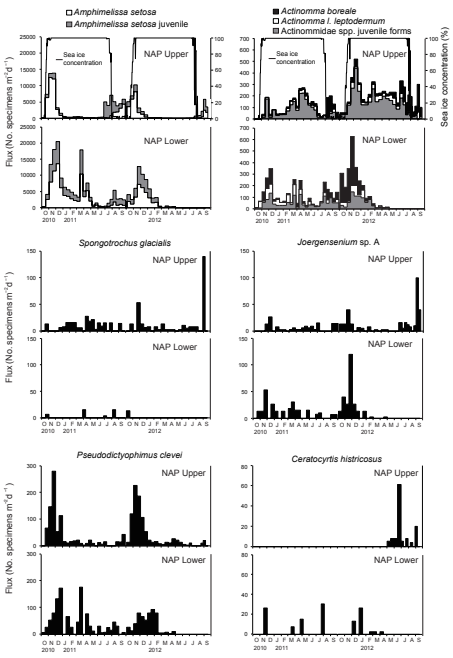

Figure 7. Two year fluxes of major radiolarian taxa at Station NAP during the sampling period.

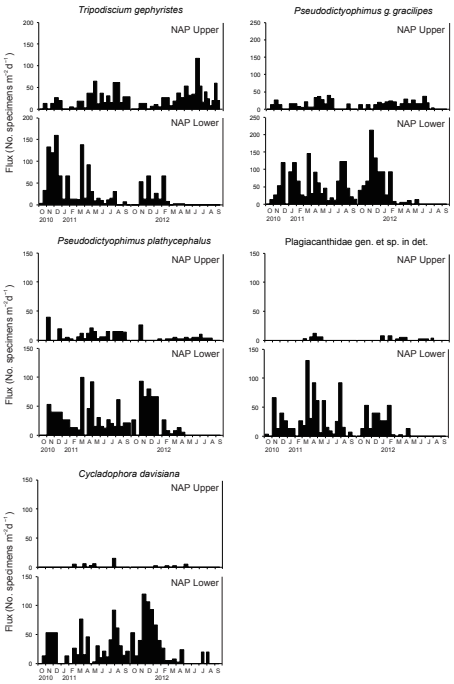

Figure 7. Continued.

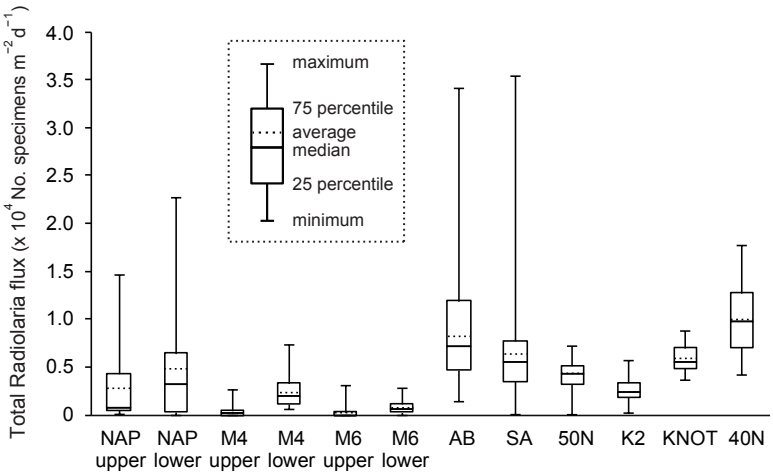

Figure 8. Box plot of total radiolarian fluxes at Station NAP and previous studied areas in the North Pacific Ocean.

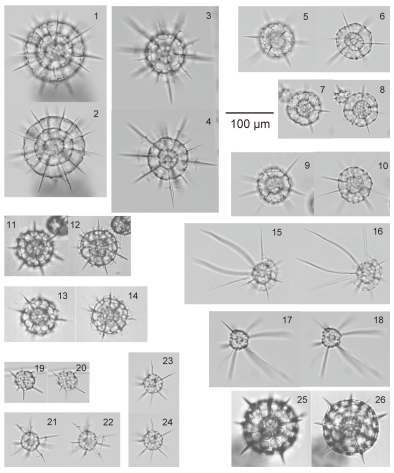

Plate 1. 1–4. *Actinomma boreale* (Cleve, 1899). 1, 2. *Actinomma boreale,* same specimen. NAP10t Shallow #23. 3, 4. *Actinomma boreale,* same specimen. NAP10t Shallow #24. 5–10. *Actinomma leptodermum leptodermum* (Jørgensen, 1900). 5, 6. *Actinomma leptodermum leptodermum,* same specimen. NAP10t Deep #12. 7, 8. *Actinomma leptodermum leptodermum,* same specimen. NAP10t Deep #12. 9, 10. *Actinomma leptodermum leptodermum,* same specimen. NAP10t Deep #12. 11–14. *Actinomma* morphogroup A. 11, 12. *Actinomma* morphogroup A, same specimen. NAP10t Deep #4. 13, 14. *Actinomma* morphogroup A, same specimen. NAP10t Deep #4. 15–18. *Actinomma leptodermum* (Jørgensen, 1900) *longispinum* (Cortese and Bjørklund, 1998). 15, 16. *Actinomma leptodermum longispinum,* same specimen. NAP10t Deep #12. 17, 18. *Actinomma leptodermum longispinum* juvenile, same specimen. NAP10t Deep #12. 19–24. Actinommidae spp. juvenile forms. 19, 20. *Actinomma* sp. in det., same specimen. NAP10t Deep #12. 21, 22. *Actinomma* sp. in det., same specimen. NAP10t Deep #12. 23, 24. *Actinomma* sp. in det., same specimen. NAP10t Deep #12. 25–26. *Actinomma turidae* (Kruglikova and Bjørklund, 2009), same specimen. NAP10t Deep #22.
Scale bar = 100 µm for all figures.

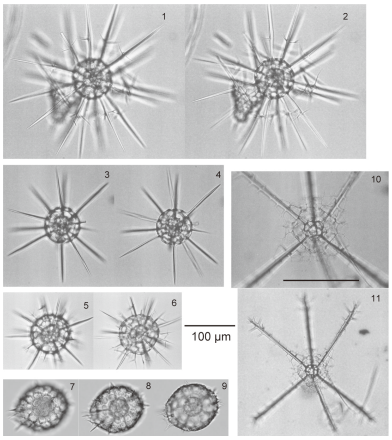

Plate 2. 1–4. *Actinomma* morphogroup B. 1, 2. *Actinomma* morphogroup B, same specimen. NAP10t Deep #4. 3, 4. *Actinomma* morphogroup B juvenile, same specimen. NAP10t Deep #15. 5, 6. *Drymyomma elegans* (Jørgensen, 1900), same specimen. NAP10t Deep #14. 7–9. *Actinomma friedrichdreyeri* (Burridge, Bjørklund and Kruglikova, 2013), same specimen. NAP11t Deep #4. 10–11. *Cleveiplegma boreale* (Cleve, 1899), same specimen. NAP11t Deep #12.
Scale bar = 100 µm for all figures.

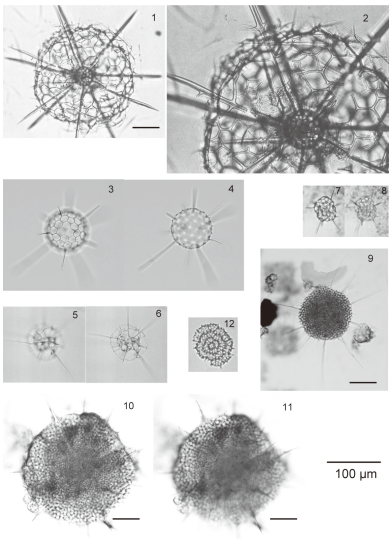

Plate 3. 1–4. *Arachnosphaera dichotoma* (Jørgensen, 1900). 1, 2. *Arachnosphaera dichotoma,* same specimen. NAP11t Deep #5. 3, 4. *Arachnosphaera dichotoma,* same specimen. NAP11t Deep #4. 5–8. *Streblacantha circumtexta*? (Jørgensen, 1905). 5, 6. *Streblacantha circumtexta*? juvenile form, same specimen NAP10t Deep #12. 7, 8. *Streblacantha circumtexta*? juvenile form, same specimen. NAP10t Shallow #23. 9–11. *Spongotrochus glacialis* (Popofsky, 1908). 9. *Spongotrochus glacialis*. NAP10t Shallow #24. 10, 11. *Spongotrochus glacialis,* same specimen. NAP10t Shallow #22. 12. *Stylodictya* sp. NAP10t Shallow #16.
Scale bar = 100 µm for all figures.

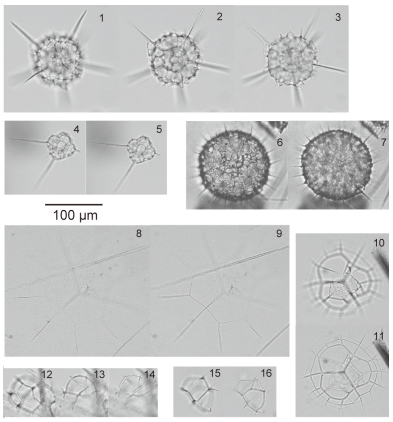

Plate 4. 1–7. *Joergensenium* spp. 1, 2, 3. *Joergensenium* sp. A, same specimen. NAP10t Deep #12. 4, 5. *Joergensenium* sp. A, juvenile forms of 1–3, same specimen. NAP11t Deep #4. 6, 7. *Joergensenium* sp. B, same specimen. NAP11t Deep #9. 8–9. *Enneaphormis rotula* (Haeckel, 1881), same specimen. NAP11t Deep #4. 10–11. *Enneaphormis enneastrum* (Haeckel, 1887), same specimen. NAP10t Deep #12. 12–16. *Protoscenium simplex* (Cleve, 1899). 12, 13, 14. *Protoscenium simplex,* same specimen. NAP10t Deep #12. 15, 16. *Protoscenium simplex,* same specimen. NAP10t Deep #12.
Scale bar = 100 µm for all figures.

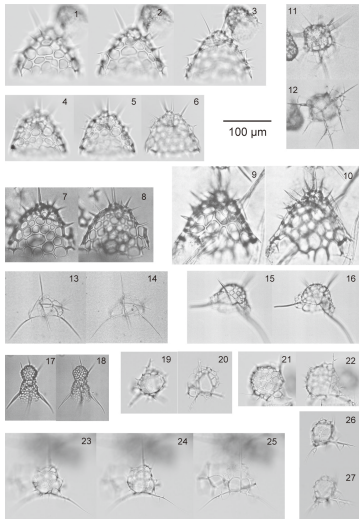

Plate 5. 1–6. *Ceratocyrtis histricosus* (Jørgensen, 1905). 1, 2, 3. *Ceratocyrtis histricosus,* same specimen. NAP10t Deep #12. 4, 5, 6. *Ceratocyrtis histricosus,* same specimen. NAP10t Deep #12. 7–10. *Ceratocyrtis galeus* (Cleve, 1899). 7, 8. *Ceratocyrtis galeus,* same specimen. NAP10t Deep #6. 9, 10. *Ceratocyrtis galeus*, same specimen. NAP10t Deep #4. 11–12. *Arachnocorys umbellifera* (Haeckel, 1862), same specimen apical view. NAP10t Deep #4. 13–16. *Cladoscenium tricolpium* (Haeckel, 1887). 13, 14. *Cladoscenium tricolpium*, same specimen. NAP10t Deep #6. 15, 16. *Cladoscenium tricolpium*?, same specimen. NAP10t Deep #14. 17–18. *Lophophaena clevei* (Petrushevskaya, 1971), same specimen. NAP10t Shallow #14. 19–27. *Phormacantha hystrix* (Jørgensen, 1900). 19, 20. *Phormacantha hystrix*, same specimen. NAP10t Deep #12. 21, 22. *Phormacantha hystrix*, same specimen. NAP10t Deep #12. 23, 24, 25. *Phormacantha hystrix*, same specimen. NAP10t Deep #12. 26, 27. *Phormacantha hystrix*, same specimen. NAP10t Deep #12.
Scale bar = 100 µm for all figures.

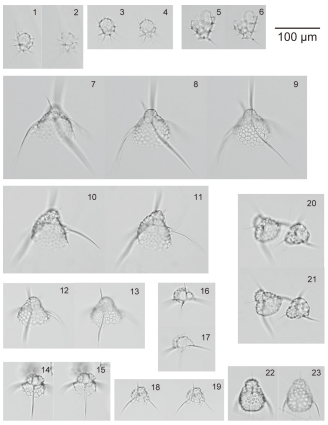

Plate 6. 1–4. *Peridium longispinum*? (Jørgensen, 1900). 1, 2. *Peridium longispinum*?, same specimen. NAP11t Deep #4. 3, 4. *Peridium longispinum*?, same specimen. NAP11t Deep #4. 5–6. *Plectacantha oikiskos* (Jørgensen, 1905), same specimen. NAP10t Deep #12. 7–11. *Pseudodictyophimus clevei* (Jørgensen, 1900). 7, 8, 9. *Pseudodictyophimus clevei*, same specimen. NAP10t Deep #12. 10, 11. *Pseudodictyophimus clevei*, same specimen. NAP10t Deep #12. 12–13. *Pseudodictyophimus gracilipes gracilipes* (Bailey, 1856), same specimen. NAP10t Deep #12. 14–19. *Pseudodictyophimus* spp. juvenile forms. 14, 15. *Pseudodictyophimus* in det., juvenile forms same specimen. NAP10t Deep #12. 16, 17. *Pseudodictyophimus* in det., juvenile forms, same specimen. NAP10t Deep #12. 18, 19. *Pseudodictyophimus* in det., juvenile forms same specimen. NAP10t Deep #12. 20–23. *Pseudiodictyophimus gracilipes* (Bailey, 1856) *bicornis* (Ehrenberg, 1861). 20, 21. *Pseudiodictyophimus gracilipes bicornis*, same specimen. NAP11t Deep #4. 22, 23. *Pseudiodictyophimus gracilipes bicornis*, same specimen. NAP11t Deep #4.
Scale bar = 100 µm for all figures.

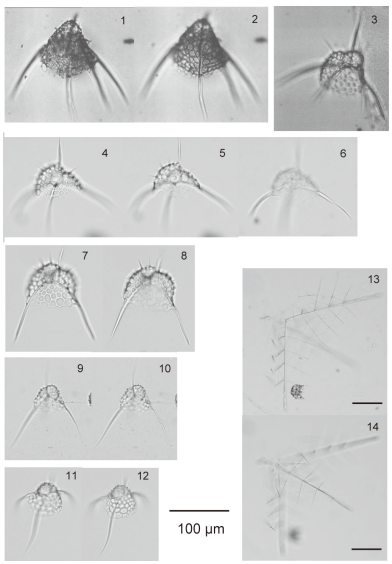

Plate 7. 1–3. *Pseudodictyophimus gracilipes* (Bailey, 1856) *multispinus* (Bernstein, 1934) 1, 2. *Pseudodictyophimus gracilipes multispinus*, same specimen. NAP10t Shallow #2. 3. *Pseudodictyophimus gracilipes multispinus.* NAP11t Shallow #2. 4–12. *Pseudodictyophimus plathycephalus* (Haeckel, 1887). 4, 5, 6. *Pseudodictyophimus plathycephalus,* same specimen. NAP10t Deep #12. 7, 8. *Pseudodictyophimus plathycephalus,* same specimen. NAP10t Deep #12. 9, 10. *Pseudodictyophimus plathycephalus,* same specimen. NAP10t Deep #12. 11, 12. *Pseudodictyophimus plathycephalus,* same specimen. NAP11t Deep #4. 13–14. *Tetraplecta pinigera* (Haeckel, 1887), same specimen. NAP10t Deep #12.
Scale bar = 100 µm for all figures.

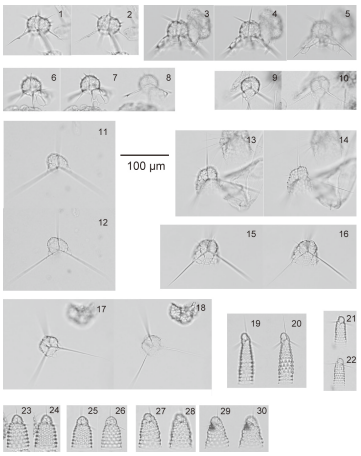

Plate 8. 1–10. *Tripodiscium gephyristes* (Hülsemann, 1963). 1, 2. *Tripodiscium gephyristes*, same specimen. NAP10t Deep #12. 3, 4, 5 *Tripodiscium gephyristes*, same specimen. NAP10t Deep #12. 6, 7, 8. *Tripodiscium gephyristes*, same specimen. NAP10t Deep #12. 9, 10. *Tripodiscium gephyristes*, same specimen. NAP10t Deep #12. 11–18. Plagiacanthidae gen. et sp. in det. 11, 12. Plagiacanthidae gen. et sp. in det. juvenile, same specimen. NAP10t Deep #12. 13, 14. Plagiacanthidae gen. et sp. in det., same specimen. NAP10t Deep #12. 15, 16. Plagiacanthidae gen. et sp. in det., same specimen. NAP10t Deep #12. 17, 18. Plagiacanthidae gen. et sp. in det. juvenile, same specimen. NAP10t Deep #12. 19–22. *Artostrobus annulatus* (Bailey, 1856). 19, 20. *Artostrobus annulatus*, same specimen. NAP10t Deep #12. 21, 22. *Artostrobus annulatus*, same specimen. NAP10t Deep #12. 23–30. *Artostrobus joergenseni* (Petrushevskaya, 1967). 23, 24. *Artostrobus joergenseni*, same specimen. NAP10t Deep #12. 25, 26. *Artostrobus joergenseni*, same specimen. NAP10t Deep #12. 27, 28. *Artostrobus joergenseni*, same specimen. NAP10t Deep #12. 29, 30. *Artostrobus joergenseni*, same specimen. NAP10t Deep #12.
Scale bar = 100 µm for all figures.

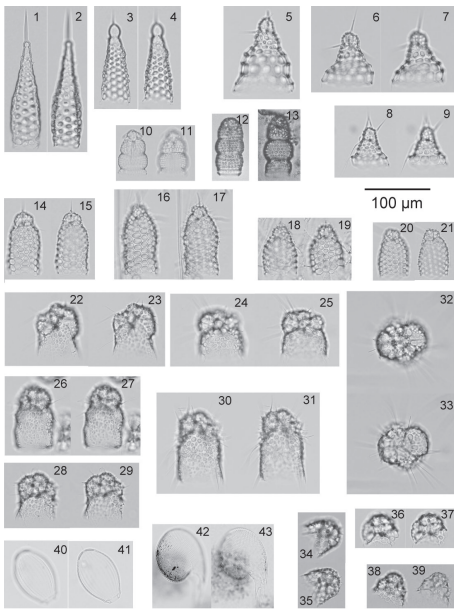

Plate 9. 1, 2. *Cornutella stylophaena* (Ehrenberg, 1854), same specimen. NAP10t Deep #12. 3, 4. *Cornutella longiseta* (Ehrenberg, 1854), same specimen. NAP10t Deep #12. 5–9. *Cycladophora davisiana* (Ehrenberg, 1862). 5. *Cycladophora davisiana*, NAP11t Deep #4. 6, 7. *Cycladophora davisiana*, same specimen. NAP10t Deep #12. 8, 9. *Cycladophora davisiana*, same specimen. NAP10t Deep #12. 10–11. *Lithocampe aff. furcaspiculata* (Popofsky, 1908). same specimen. NAP10t Deep #12. 12–13. *Lithocampe platycephala* (Ehrenberg, 1873). 12. *Lithocampe platycephala*. NAP10t Deep #13. 13. *Lithocampe platycephala*. NAP11t Deep #14. 14–21. *Sethoconus tabulatus* (Ehrenberg, 1873). 14, 15. *Sethoconus tabulatus*, same specimen. NAP10t Deep #12. 16, 17. *Sethoconus tabulatus*, same specimen. NAP10t Deep #12. 18, 19. *Sethoconus tabulatus*, same specimen. NAP10t Deep #12. 20, 21. *Sethoconus tabulatus*, same specimen. NAP10t Deep #12. 22–33. *Amphimelissa setosa* (Cleve, 1899). 22, 23. *Amphimelissa setosa*, same specimen. NAP10t Deep #12. 24, 25. *Amphimelissa setosa*, same specimen. NAP10t Deep #12. 26, 27. *Amphimelissa setosa*, same specimen. NAP10t Deep #12. 28, 29. *Amphimelissa setosa*, same specimen. NAP11t Deep #4. 30, 31. *Amphimelissa setosa*, same specimen. NAP10t Deep #12. 32, 33. *Amphimelissa setosa*, same specimen, apical view. NAP11t Deep #4. 34–39. *Amphimelissa setosa* juvenile. 34, 35. *Amphimelissa setosa* juvenile, same specimen. NAP11t Deep #14. 36, 37. *Amphimelissa setosa* juvenile, same specimen. NAP10t Deep #12. 38, 39. *Amphimelissa setosa* juvenile, same specimen. NAP11t Deep #14. 40–41. *Lirella melo* (Cleve, 1899), same specimen. NAP10t Deep #14. 42–43. *Protocystis harstoni* (Murray, 1885), same specimen. NAP10t Deep #18.
Scale bar = 100 µm for all figures.